nature portfolio

Peer Review File

High-efficiency atmospheric water harvesting enabled by ultrasonic extraction

Corresponding Author: Dr Svetlana Boriskina

This file contains all reviewer reports in order by version, followed by all author rebuttals in order by version.

Version 0:

Reviewer comments:

Reviewer #1

(Remarks to the Author)
In this work, the authors introduce a novel method for moisture extraction utilizing vibrational mechanical actuation enabled by piezoelectric materials. Although the authors have conducted extensive research on this approach, they have not sufficiently demonstrated its significance and potential applications. While some key points are addressed in the discussion section, such as comparisons with photothermal methods and the practicality and universality of the technique, these claims lack supporting experimental evidence, making it difficult to substantiate the method's promise. Specific comments are as follows:
(1) In the discussion section (Page 16), the authors compare their method with photothermal techniques, stating that the current photothermal conversion efficiency limit is only 15%. Despite providing references, this argument appears to be inaccurate. The authors failed to provide an objective comparison and clearly demonstrate the uniqueness of their method.
(2) On page 17, the authors use limited experimental data to estimate the water yield of their devices at 1 m^2, which is insufficient to convince readers of its effectiveness on larger scales. While the proposed method works well for small samples, the challenge of internal water drainage increases with sample size. How does this method perform on large-scale samples?
(3) The authors mention the applicability of their method to other material systems, yet it would be beneficial to provide experimental data to support this claim.
(4) Vibration-induced moisture extraction can indeed reduce energy consumption compared to thermal methods. However, it also results in more water being expelled through small droplets or water clusters, potentially carrying ions or micro-nanoparticles from the material, leading to deteriorated water quality.

Reviewer #2

(Remarks to the Author)
In this work, the authors demonstrate that vibrational mechanical actuation can be used instead of heat to extract water from moisture harvesting materials, offering about five-fold increase in the extraction energy efficiency. However, some revisions need to be made before publication. My comments are below:
(1) The efficiency is the critical index of the atmospheric water harvester. I suggest the authors to provide the detailed calculation process.
(2) Figure 2(d) and (e) show the SEM image of images of HG-A and HG-C samples, respectively. The figures lack scale bar.
(3) How stable is the proposed atmospheric water harvester? Does it work for a long time?
(4) To further facilitate practical application, it is necessary to carry out economic analysis.

Reviewer #3

(Remarks to the Author)
This work demonstrates the use of a combined ultrasonic actuator and heating to induce desorption of water from a sorbent for atmospheric water harvesting. While the work is interesting and well supported, the following questions/comments need to be addressed:

- The comparison of performance with and without the piezoelectric actuator shows that this approach can be used with a lower energy consumption than the tradition heating-induced evaporation. In many ways, this is analogous to a comparison between ultrasonic and evaporative humidifiers that are commercially available. Furthermore, there are papers on using ultrasound to trigger controlled release from hydrogels for biomedical applications. So, the authors should better explain the novelty of their work.
- The authors refer to a thermodynamic limit and claim that the device is not bound by that – how is this claim made? They may be referring to a thermal "limit", but by definition the thermodynamic limit is agnostic to the process (it can be a blackbox).
- How is Q_e calculated for the efficiency given that the energy input is electricity? In general, a better explanation of the 10% efficiency for "state-of-the-art" devices and the 47% efficiency of the current device is needed. Is the comparison really 1-1?
- Some more clarification on the separate and coupled effects of mechanical actuation vs. heating can be included to better explain the results.
- The last section on discussion and outlook seems to take a different turn and not fit within the current scope, so it is suggested to better integrate this or remove it.
- Projecting results from a 0.0002 m2 device that produced 0.11 mL of water to a 1 m2 device needs to be better justified. Transport properties do not scale linearly, and fluctuations in ambient conditions (diurnal or seasonal) will have an impact. Furthermore, a MEMS-inspired device is used for the demonstration and it is not clear how that will be scaled, and what impact that has on cost.
- The last sentence says "breaking the thermal efficiency limit" which is not a 1-1 comparison since the proposed approach does not use only a thermally induced desorption.
- Is there any data on the repeatability of using the approach, or does the vibration degrade the gel mechanics over many cycles?

Version 1:

Reviewer comments:

Reviewer #2

(Remarks to the Author)
The authors handled all my concerns. Now the manuscript can be accepted in the present form.

Reviewer #4

(Remarks to the Author)
I have carefully reviewed the manuscript by Shuvo and Boriskina et al. before considering the comments and suggestions raised by the other reviewers in the previous review cycle. This work does report an interesting phenomenon in the field of atmospheric water harvesting (AWH) that water can be extracted from a hydrogel by using an ultrasonic actuator. The authors convincingly demonstrated that they are attempting to address one of the major challenges in the field: the optimization of energy consumption for sorbent regeneration and freshwater production. However, I also have similar concerns to other reviewers in terms of energy consumption and calculations, water qualities, scalabilities, etc., even though with the resubmitted manuscript.
1. It is known that the thermally-driven sorbent regeneration and freshwater production systems can make direct use of low-grade energy, such as waste heat, or thermal energy converted from solar energy. The ultrasonic water extraction reported in this work relies entirely on electricity, a high-grade secondary energy and substantial energy losses occur during electricity generation. For example, commercial PV modules normally converts only ~15-20% of incident energy in practice while thermal power plant converts approximately 30-40% of energy from burning fossil fuels. If these upstream losses are counted, the ultrasonic route suffers a three- to five- fold increases in primary energy demand and a correspondingly larger carbon footprint.
2. The daily freshwater yield of the ultrasonic approach is projected at around 3.2 L m^{-2} day^{-1}; by contrast, the state-of-the-art solar-thermal systems already deliver much higher productivity, for example, 3.65 L/m2/day (Energy Environ. Sci., 2024, 17, 4988-5001), 3.5-8.9 L/m2/day (Nat. Commun. 2024, 15, 7678), 5.02 L/m2/day (Adv. Funct. Mater. 2025, 2501163), etc., by using only solar energy. It is premature to conclude that ultrasonic-driven process outperforms its thermal-based counterparts.
3. Another critical question is whether AWH remains advantageous when scaled to grid-connected systems. At a relative humidity of 75 %, a level the experiment of this work carried out for freshwater productivity prediction, AWH can indeed produce water. However, the availability of grid electricity removes the energy constraint that AWH is designed to circumvent. Under such conditions, conventional condensation technologies (e.g., dehumidifiers) are likely to deliver significantly higher water yields and should be evaluated as the more favorable option than the ultrasonic approach.
4. The measured energy demand falls below the latent-heat limit, implying that water is released as clusters or micro-droplets rather than as pure vapor. This mechanism can entrain salt ions and polymer fragments—ranging from nano- to micro-scale—during extraction. Such particles are invisible to routine analytical methods yet still pose potential health risks. Consistent with this picture, the collected water contains 1.5–15.2 ppm of lithium ions, confirming that lithium chloride was carried out of the sorbent together with the harvested water.
5. The long-term stability could be a major challenge in this actuator-hydrogel-based AWH system. Lithium chloride aggressively corrodes most metals, threatening ultrasonic device integrity, so the claimed 25-year service life is almost

certainly an overestimate. Equally uncertain is the hydrogel itself: its mechanical strength, degree of polymerization, and resistance to cyclic swelling must be monitored over thousands of operating cycles. The current durability test, only a 25–30 % duty cycle over 45 min, falls far short of demonstrating a 30-day lifespan. These unresolved reliability issues also cast doubt on the projected cost target of $0.19 L^{-1}
6. Noise pollution represents an additional, often-overlooked challenge, particularly for scaled-up arrays capable of meeting an adult's daily water requirement. A single ultrasonic actuator poses little risk to human health, yet hundreds operating in close proximity can create an ultrasound level that may compromise comfort and well-being; this collective impact must be explicitly evaluated and mitigated.

Version 2:

Reviewer comments:

Reviewer #4

(Remarks to the Author)
The authors addressed my comments satisfactorily and I thus recommend its acceptance.

Response to the reviewers for manuscript:

High-efficiency atmospheric water harvesting enabled by ultrasonic extraction

by

Ikra Shuvo[1], Carlos D. Díaz-Marín[2], Marvin Christen[4], Michael Lherbette[4], Christopher Liem[3], Svetlana V. Boriskina[2]*

[1]*Media Lab, Massachusetts Institute of Technology, Cambridge, MA 02139, USA*

[2]*Department of Mechanical Engineering, Massachusetts Institute of Technology, Cambridge, MA 02139, USA*

[3]*Department of Electrical Engineering and Computer Science, Massachusetts Institute of Technology, Cambridge, MA 02139, USA*

[4]*SmarAct Metrology GmbH & Co. KG, Oldenburg, HRA 207391, Germany.*

*Corresponding author: sborisk@mit.edu

We are grateful for the constructive comments from the reviewers on our manuscript. The reviewer's comments are in blue, with our responses for each specific comment below. The text that has been added to the revised manuscript is colored red. To properly address the repeating comments from multiple reviewers, we added several new Supplementary Notes to the revised version of the manuscript. These notes (4-8) are included at the bottom of this letter and are referenced in our responses below to avoid duplicating large portions of the text.

Reviewer#1

In this work, the authors introduce a novel method for moisture extraction utilizing vibrational mechanical actuation enabled by piezoelectric materials. Although the authors have conducted extensive research on this approach, they have not sufficiently demonstrated its significance and potential applications. While some key points are addressed in the discussion section, such as comparisons with photothermal methods and the practicality and universality of the technique, these claims lack supporting experimental evidence, making it difficult to substantiate the method's promise. Specific comments are as follows:

(1) In the discussion section (Page 16), the authors compare their method with photothermal techniques, stating that the current photothermal conversion efficiency limit is only 15%. Despite providing references, this argument appears to be inaccurate. The authors failed to provide an objective comparison and clearly demonstrate the uniqueness of their method.

We thank the reviewer for raising this important point and would like to clarify some confusion about the efficiency of different processes discussed in the manuscript.

(i) The photothermal conversion efficiency discussed on page 16 is the **efficiency of solar-thermal energy conversion**, which is compared to the **efficiency of photovoltaic solar energy conversion process**. Our method of water extraction can use electrical energy from the grid, from a stand-alone PV cell, or from any local generator. The conventional method of thermal moisture extraction via evaporation can use solar energy directly by absorbing it and converting it to heat, which may create an impression that this is a more efficient energy conversion process. However, the efficiency of solar energy conversion to electricity in a PV cell is ~20-25%, while solar-thermal energy conversion efficiency under unconcentrated sunlight is lower (~15%) because of the heat losses via thermal re-emission. The argument above was included to explain the point that although the vibrational extraction technique requires energy input in the form of electricity, while thermal extraction can use sunlight directly, direct solar heat usage for thermal extraction not offer any advantage from the energy efficiency standpoint over the PV cell. If the electrical energy from the grid is used, the above argument is completely irrelevant.

(ii) More importantly, **neither of the efficiencies above should be directly compared to the energy efficiency of the water extraction**, which is the central point of our study. The electrical energy supplied to our actuator-sorbent system can be generated by any [unspecified] method, and only the total electric energy input to the system is used to calculate the water extraction efficiency. In our lab experiments, the electrical energy is supplied from the grid.

To avoid unnecessary confusion, and also following the recommendation of Reviewer 3, we significantly shortened this discussion, which is outside of the main scope of the manuscript.

(iii) At the same time, to clarify the definition and calculations of **the energy efficiency of the water release process** (which is ambivalent to the source of the energy and is the central point of this work), we have added **Supplementary Note 4** to the Supporting Information.

After including the new data summarized in **Table S4**, the revised **Fig. 1e** is as follows:

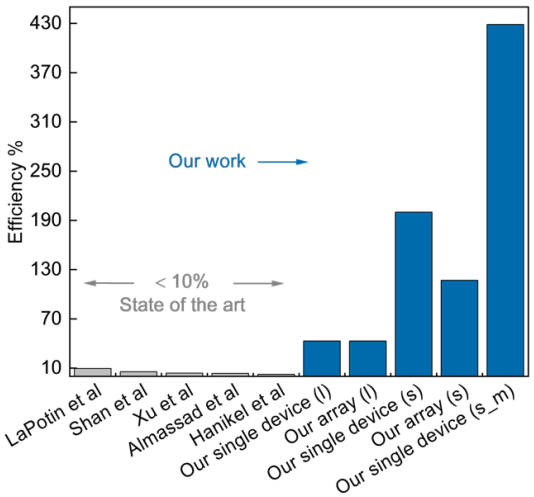

Figure 1e: Efficiency values of the moisture extraction achieved in this study compared with the state-of-the-art literature data (here, s = short actuation period; l= long actuation period; s_m = multiple repetitive cycles of short actuation periods).

Similarly, the revised **Fig. 6d** (previously **Fig. 6c)** portraying the energy consumption of the devices is as follows:

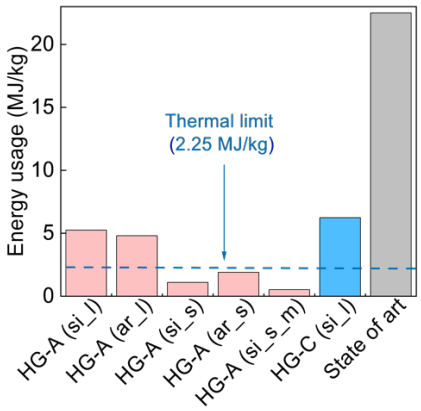

Figure 6d: A comparative analysis of energy consumption between actuator-enabled water extraction and the state-of-the-art thermally driven evaporation process [1] (here, si_l = a single device actuated over a long period; ar_l = an array of devices actuated over a long period; si_s = a single device actuated over a short period; ar_s = an array of devices actuated over a short period; si_s_m = a single device actuated over multiple short periods).

(2) On page 17, the authors use limited experimental data to estimate the water yield of their devices at 1 m², which is insufficient to convince readers of its effectiveness on larger scales. While the proposed method works well for small samples, the challenge of internal water drainage increases with sample size. How does this method perform on large-scale samples?

We agree with Reviewer #1 that, in general, the efficiency and productivity of a scaled-up system will be very specific in each implementation and would need to be evaluated on the case-by-case basis. Our statement is based on the simplest scaling strategy, which assumes that **multiple identical actuators with hydrogel samples identical to those used in our study will be deployed in the form of a 2D array with the total area of the sample surface equal to m^2.** We further assume that each actuator will be powered separately and the energy consumption per device will be the same as measured in our experiments. This is likely not the most efficient way of scaling the system up and would overestimate the daily energy consumption of the system and underestimate the energy efficiency of extraction. We added **Supplementary Note 5** to the manuscript to explain how the daily yield and energy efficiency of extraction is estimated for a scaled-up system.

The following text has been added to the Discussion section of the manuscript:

We estimated the daily yield of water that can be harvested from a scaled-up system with a 1-m^2 sorbent area [L/m²/day] by extrapolating the results of cyclic sorption-desorption testing of a single prototype device with a large sorbent over 10 hours at 75% RH, i.e., by using the data shown in **Fig. 6c**. This simple scaling strategy assumes that multiple identical actuators with hydrogel

samples identical to those used in our study are deployed in the form of a 2D array with the total area of the sample surface equal to 1 m^2. We further assumed that each actuator is powered separately and the energy consumption per device is the same as measured in our experiments. The resulting average daily productivity value has been predicted to be ~3.2 [L/m^2/day], and the average device extraction efficiency - 0.576 MJ/kg (see Supplementary Note 5).

This is likely not the most efficient way of scaling the system up and overestimates the daily energy consumption while underestimating the energy efficiency of extraction. The effectiveness of large-area PZT-based ultrasound transduction has been demonstrated in various unrelated studies. For example, an interconnected network comprising hundreds of miniaturized PZT actuators has been employed over a 20cm x 20cm area, utilizing only 6W of electric power, resulting in efficient transduction intensity at a depth up to 8mm^2. Similarly, larger piezoelectric components could be utilized in arrays, akin to those employed in sonar applications for underwater wireless communication, which are inherently designed with a larger footprint area extending up to several sq. feet[3]. Future research could implement these strategies to test the AWH sorbents with a custom-made actuator array over a large surface area and associated electronic circuits for optimum power supply to the array. We expect that scaling laterally through arrays of multiple piezoelectric devices, while maintaining hydrogel thickness within a few millimeters, may yield even better performance and higher energy efficiency than we predict based on the simple approach described above.

(3) The authors mention the applicability of their method to other material systems, yet it would be beneficial to provide experimental data to support this claim.

We thank the reviewer for raising this important point. The discussion section of the manuscript has been modified to include the following text:

In our study, we demonstrate the approach applicability to extract moisture with high efficiency from two different hydrogel systems. These results give reason to expect that ultrasound actuation can facilitate moisture extraction from other sorbents. This hypothesis is independently supported by literature evidence on increased drying rate of textiles[4], seaweed[5], and zeolite[6] under ultrasonic actuation. Each material system would need to be evaluated separately under optimized actuation conditions, moisture content, and sorbent geometry, which will be a subject of our future work.

(4) Vibration-induced moisture extraction can indeed reduce energy consumption compared to thermal methods. However, it also results in more water being expelled through small droplets or water clusters, potentially carrying ions or micro-nanoparticles from the material, leading to deteriorated water quality.

We addressed this important concern by adding the following **Supplementary Notes 6 and 7** that describe the material stability and extracted water quality testing. The Method section has also been revised to include the information on the testing methodology.

The following paragraph has been added to the Methodology section:

Li content test of extracted water

Agilent 5100 DVD was used to test the quality of the ultrasonically-extracted water from PAM-LiCl hydrogels via a coupled plasma optical emission spectrometer (ICP-OES) elemental analysis, similar to the test methods reported in recent studies of AWH hygroscopic gels[7]. Prior to testing with the Agilent 5100 DVD, the extracted water was collected using VWR sterile syringe filters. Multiple desorbed specimens were tested.

Reviewer #2

In this work, the authors demonstrate that vibrational mechanical actuation can be used instead of heat to extract water from moisture harvesting materials, offering about five-fold increase in the extraction energy efficiency. However, some revisions need to be made before publication. My comments are below:

(1) The efficiency is the critical index of the atmospheric water harvester. I suggest the authors to provide the detailed calculation process.

We thank the reviewer for raising this important point. Please refer to the **Supplementary Note 4 – Efficiency calculation of the device** at the bottom of this letter for the detailed calculation process.

(2) Figure 2(d) and (e) show the SEM image of images of HG-A and HG-C samples, respectively. The figures lack scale bar.

We have included the scale bar into the Figure 2 panel, thank you for pointing out this omission.

(3) How stable is the proposed atmospheric water harvester? Does it work for a long time?

The AWH hydrogel sorbent used in this work has been previously demonstrated to have high cycling stability under thermal moisture extraction operation[8]. The original version of the manuscript showed stable cycling performance of our system with hydrogels and ultrasonic extraction for three extraction cycles. To address the material stability during operation over a longer time, we have conducted additional cyclic sorption-extraction experiments over the course of 8-10 hr (see **Figs. 6c, S36, S37 and Supplementary Note 5)**. Each cycle included exposure of the sorbent to air at 75% relative humidity for 1 hour, followed by 2 minutes of ultrasonic extraction with 25% duty cycle. Our previous experiments indicated that the desorption rate (and thus energy efficiency) declines after the initial few minutes of ultrasound actuation. To prevent such efficiency degradation and to operate close to the optimum extraction conditions, we implemented shorter 2-min desorption periods. These experiments allowed us to further reduce the specific energy consumption to the level below the thermal limit, as illustrated in **Figs. 6c, S36, and S37.** Furthermore, our data reveal that after 10 cycles, there was no significant degradation in performance of multiple tested samples during either water uptake or desorption periods. Please refer to the **Supplementary Note 5 – Scaled-up AWH system performance estimate** at the bottom of this letter for the detailed description and the results of the cyclic experiment.

(4) To further facilitate practical application, it is necessary to carry out economic analysis.

We thank the reviewer for the valuable recommendation and have included the technoeconomic analysis in **Supplementary Note 8**.

The following text has also been added to the discussion section:

Finally, our preliminary technoeconomic analysis of the scaled-up system performance indicates the viability of commercializing our system, with the estimated cost of water of 0.19 $/L, which is lower than the cost of bottled water in various countries worldwide, including USA, UK, Canada and Australia (see Supplementary Notes 7-9 and Supplementary Fig. S41).

Reviewer#3

This work demonstrates the use of a combined ultrasonic actuator and heating to induce desorption of water from a sorbent for atmospheric water harvesting. While the work is interesting and well supported, the following questions/comments need to be addressed:

(1) The comparison of performance with and without the piezoelectric actuator shows that this approach can be used with a lower energy consumption than the tradition heating-induced evaporation. In many ways, this is analogous to a comparison between ultrasonic and evaporative humidifiers that are commercially available. Furthermore, there are papers on using ultrasound to trigger controlled release from hydrogels for biomedical applications. So, the authors should better explain the novelty of their work.

As we acknowledge in the manuscript, we do draw the inspiration from the ultrasonic water atomizers for humidification and medical applications. These applications apply ultrasound to atomize bulk water or extract drugs from over-saturated medical hydrogels with very high free water content. The novelty of our work is in the application of piezo-induced actuation technology for water extraction from AWH sorbents, which have low moisture content, making efficient extraction much more challenging. The conventional method that has been used so far by the AWH technology is thermal evaporation and condensation, which is a very energy-intensive process. Our work offers the first ever (to the best of our knowledge) experimental demonstration of the energy consumption of such process below the enthalpy of water evaporation (referred to as the thermal limit). This major improvement in energy efficiency may significantly support AWH technology commercialization. We also expect our work to stimulate future studies on understanding the fundamental mechanisms of ultrasound interaction with different sorbents and different types of hydrogen bonds.

The preceding section (in red font) has been incorporated into the manuscript's discussion section.

(2) The authors refer to a thermodynamic limit and claim that the device is not bound by that – how is this claim made? They may be referring to a thermal "limit", but by definition the thermodynamic limit is agnostic to the process (it can be a blackbox).

Thank you for pointing out this unfortunate typo; we intended to refer to the "thermal limit" as defined in **Supplementary Note 4** at the bottom of this letter. The thermal limit is conventionally defined as the enthalpy of water evaporation process and our device – which uses non-thermal method of extraction of liquid water as well as water vapor – is not bound by this limit.

(3) How is Q_e calculated for the efficiency given that the energy input is electricity? In general, a better explanation of the 10% efficiency for "state-of-the-art" devices and the 47% efficiency of the current device is needed. Is the comparison really 1-1?

We thank the reviewer for raising this important point. We have added **Supplementary Note 4** to the Supporting Information (see above) to clarify the definition and calculations of efficiency. In short, the comparison is indeed done on equal footing. All the compared energy consumption values (and the corresponding energy efficiency values) represent the experimentally measured system-level performance data for each system, i.e., the energy consumption is measured as **the total energy input** to each system to drive the moisture extraction process. While different compared systems may have different levels of parasitic losses, only the total energy input is used in the energy calculations, allowing us to provide a 1-1 comparative estimate.

(4) Some more clarification on the separate and coupled effects of mechanical actuation vs. heating can be included to better explain the results.

We have conducted an additional experiment to elucidate the effects of mechanical actuation and heating, which are discussed in **Supplementary Note 9**.

The following sentence has been atted to the manuscript:

In our devices, we estimate the energy consumption to be roughly equally divided between the mechanical actuation (49%) and heating (51%), see Supplementary Note 9.

(5) The last section on discussion and outlook seems to take a different turn and not fit within the current scope, so it is suggested to better integrate this or remove it.

We have removed this discussion from the revised manuscript to keep the focus on our results and avoid confusion.

(6) Projecting results from a 0.0002 m2 device that produced 0.11 mL of water to a 1 m^2 device needs to be better justified. Transport properties do not scale linearly, and fluctuations in ambient conditions (diurnal or seasonal) will have an impact. Furthermore, a MEMS-inspired device is used for the demonstration and it is not clear how that will be scaled, and what impact that has on cost.

Supplementary Note 5 has been incorporated into the Supporting Information to estimate the daily water yield of a single device from the new cyclic measurements over the course of 8 to 10 hr and to extrapolate it to an array of identical devices with the total lateral area of 1m^2. Under this scaling scenario, all the actuators and all the hydrogel samples are identical to those measured in the manuscript, so transport properties would be also identical. We complemented this theoretical estimate by the experimental data on an array of three identical devices operated simultaneously.

We acknowledge in the revised version of the manuscript that this estimate is done for harvesting at ambient temperature of 24-25^{o}C and at 75% humidity, and daily variations in either temperature or RH may change this value. However, our results demonstrate that with the newly demonstrated vibrational extraction mechanism, the daily water yield is limited only by the hydrogel sorption efficiency, while the extraction step takes a small fraction of the total cycle time. This allows us to increase the productivity of each sorbent by allowing harvesting during the day as well as overnight.

We have additionally performed a technoeconomic analysis to evaluate the cost of water as a function of the actuator lifetime (see **Supplementary Note 8)**.

The following text has been added to the discussion section:

We estimated the daily yield of water that can be harvested from a scaled-up system with a 1-m^2 sorbent area [L/m^2/day] by extrapolating the results of cyclic sorption-desorption testing of a single prototype device with a large sorbent over 10 hours at 75% RH, i.e., by using the data shown in **Fig. 6c**. This simple scaling strategy assumes that multiple identical actuators with hydrogel samples identical to those used in our study are deployed in the form of a 2D array with the total area of the sample surface equal to 1 m^2. We further assumed that each actuator is powered separately and the energy consumption per device is the same as measured in our experiments. The resulting average daily productivity value has been predicted to be ~3.2 [L/m^2/day], and the average device extraction efficiency - 0.576 MJ/kg (see Supplementary Note 5). This is likely not the most efficient way of scaling the system up and overestimates the daily energy consumption while underestimating the energy efficiency of extraction.

(7) The last sentence says “breaking the thermal efficiency limit” which is not a 1-1 comparison since the proposed approach does not use only a thermally induced desorption.

We have revised the statement to clearly articulate the fact that by using the vibrational extraction mechanism, we demonstrated the specific energy consumption below that prescribed by the thermal limit (defined as the enthalpy of water vaporization). This results in the conventionally-defined energy efficiency values in excess of 100%, which is fundamentally

allowed because the concept of the thermal limit does not apply to a non-thermal extraction process (such as vibrational actuation).

(8) Is there any data on the repeatability of using the approach, or does the vibration degrade the gel mechanics over many cycles?

The AWH hydrogel sorbent used in this work has been previously demonstrated to have high cycling stability under thermal moisture extraction operation[8]. The original version of the manuscript showed stable cycling performance of our system with hydrogels and ultrasonic extraction for three extraction cycles. To address the material stability during operation over a longer time, we have conducted additional cyclic sorption-extraction experiments over the course of 8-10 hr (see **Figs. 6c, S36, S37 and Supplementary Note 5)**. Each cycle included exposure of the sorbent to air at 75% relative humidity for 1 hour, followed by 2 minutes of ultrasonic extraction with 25% duty cycle. Our previous experiments indicated that the desorption rate (and thus energy efficiency) declines after the initial few minutes of ultrasound actuation. To prevent such efficiency degradation and to operate close to the optimum extraction conditions, we implemented shorter 2-min desorption periods. These experiments allowed us to further reduce the specific energy consumption to the level below the thermal limit, as illustrated in **Figs. 6c, S36, and S37.** Furthermore, our data reveal that after 10 cycles, there was no noticeable degradation in performance of multiple tested samples during either water uptake or desorption periods. Please refer to the **Supplementary Note 5 – Scaled-up AWH system performance estimate** at the bottom of this letter for the detailed description and the results of the cyclic experiment.

The following text has been added to the manuscript:

The lowest energy consumption of 0.48 MJ/kg has been recorded for the extraction from the largest 34-mm-diameter sample, for which cyclic sorption-desorption testing over 10 hours has been performed, with ten 1-hour-long sorption cycles run at 75% RH, separated by eleven 2-minute-long extraction cycles. **Fig. 6c** shows the extracted water mass and energy efficiency for each extraction cycle.

Supplementary Notes added to the revised version of the manuscript

1.4. Supplementary Note 4 – Efficiency calculation of the device

The efficiency of the water release process, η, was calculated as [9] [10]:

$$\eta = \frac{h_{lv}}{E} \times 100\%$$

where $h_{lv} = 2.257$ [MJ/kg] is the enthalpy of vaporization of water and E [MJ/kg] is the specific energy consumption defined as the energy input (electrical, thermal, or a combination thereof, depending on each individual system configuration) divided by the mass of water released from a sorbent. In an ideal thermal process, all the heat provided to the system is used to evaporate water i.e., $E = h_{lv}$, where it is also considered that the enthalpy of desorption is identical to the enthalpy of vaporization of water. Therefore, an ideal thermal process has $\eta = 100\%$. In this work, we refer to this ideal thermal process with $\eta = 100\%$ as the thermal limit. In a real thermal water release process, the heat provided is used not only evaporate water, but also to sensibly heat the system and sorbent, and is partially lost to the ambient, leading to $\eta < 100\%$.

For our experiments, the energy consumption (E) after the weight-loss experiment was calculated using the following equation, where P is input energy, m is the output extracted weight or amount of weight loss measured in g, and $1\ Wh = 3.6 \cdot 10^3\ J$:

$$E\left[\frac{MJ}{kg}\right] = \frac{P}{m} = \frac{\text{Supplied power } [MJ]}{m\ [kg]} = \frac{V[V] \cdot I[A] \cdot \text{Actuation time } [h] \cdot \text{Duty cycle} \cdot 3.6\left[\frac{J}{Wh}\right] \cdot 10^3}{m\ [g] \cdot 10^{-3}}$$

As an example, when we applied 5 V and 0.3 A at 70% duty cycle for 10 min (~0.17 hr) using our piezoelectric actuator to desorb water from HG-M (Fig. 4E), the weight loss was measured to be 0.13 ± 0.002 g. Then, the energy consumption per unit mass of water extracted can be calculated as:

$$E = \frac{5[V] \cdot 0.3[A] \cdot 0.17\ [h] \cdot 0.7 \cdot 3.6\left[\frac{J}{Wh}\right] \cdot 10^3}{0.13\ [g] \cdot 10^{-3}} = 4.84\left[\frac{MJ}{kg}\right] = 1.35\ \left[\frac{kWh}{kg}\right]$$

Then, the efficiency of the water release process, η, can be calculated as:

$$\eta = \frac{h_{lv}}{E} \times 100\% = \frac{2.25\left[\frac{MJ}{kg}\right]}{4.84\ \left[\frac{MJ}{kg}\right]} \times 100\% = \sim 46.4\%$$

Note that this is the device-level energy efficiency, which explicitly captures all the energy losses during the extraction system operation. In the manuscript, we demonstrate that this efficiency depends on the actuation time and decreases during longer actuation periods. Cycling testing of

the system under different actuation periods revealed that short actuation times (2 minutes) yield the highest extraction energy efficiency and even allow energy consumption lower than the thermal limit.

We compared our results with the specific energy consumption E and moisture extraction energy efficiency η data for several experimentally demonstrated atmospheric water harvesting systems[9]. These values are summarized in **Table S4**, which is shown below. The table also shows the estimates of the moisture extraction efficiency per unit mass per day. Note that, unlike the specific energy consumption E and extracted water mass m, the daily values E_d and m_d are either measured over a daily collection/extraction cycle or estimated by accounting the time needed to collect the moisture from the atmosphere before it can be extracted. All the values in the table represent the experimentally obtained system-level performance data in a daily harvesting cycle and, as such, can be compared on equal footing.

Note that under the above standard definition of the efficiency (η) of AWH systems, an efficient non-thermal extraction method can have a specific energy consumption lower than the enthalpy of vaporization of water, h_{lv}. In this case, the energy efficiency of the water release process can exceed 100%. This is the case measured and reported in our manuscript, which we describe as 'breaking the thermal limit.'

2.4. Supplementary Table 4. A summary of variables derived from different literatures to derive specific energy consumption and the efficiency of the devices for water release process in comparison to our devices.

Reference	Water production (kg/day)	Energy input (kWh/day)	Specific energy consumption (kWh/kg)	Efficiency η (%)
LaPotin et al. [1]	0.06	0.421	7.02	9.5
Hanikel et al. [11]	0.41	10.79	26.32	2.4
Xu et al. [12]	0.023	0.36	15.65	4.0
Shan et al. [13]	0.311	3.475	11.17	5.6
Almassad et al. [14]	0.72	12.456	17.3	3.6
This work for HG-M[a]	0.00013*	0.000175*	1.35	47
This work for HG-A[b]	0.00013*	0.000188*	1.44	43
This work for HG-A[c]	0.00014*	0.000188*	1.44	43
This work for HG-A[d]	0.00004*	0.000013*	0.31	200
This work for HG-A[e]	0.00007*	0.000038*	0.54	117
This work for HG-A[f]	0.00094	0.000138	0.15	428.6

* Per cycle

[a] After 10-min actuation cycle using a single device

[b] After 25-min actuation cycle using a single device

[c] After 10-min actuation cycles using an array made of three devices

[d] After 2-min actuation cycle using a single device

[e] After 2-min actuation cycle using an array made of three devices

[f] Measured over 11-hr period utilizing a large specimen and eleven 2-min actuation cycles (i.e., 22 min over 11hr)

1.5. Supplementary Note 5 – Scaled-up AWH system performance estimate

To evaluate the daily water yield and energy efficiency of extraction for an AWH device scaled to the 1-m^2 area, we implemented the simplest scale-up strategy, which assumes that multiple identical actuators with hydrogel samples identical to those used in our study will be deployed in the form of a 2D array with the total area of the sample surface equal to 1 m^2. We further assume that each actuator will be powered separately and the energy consumption per device will be the same as measured in our experiments. This is likely not the most efficient way of scaling the system up and would overestimate the daily energy consumption of the system and underestimate the energy efficiency of extraction.

To illustrate the validity of the simple scaling-up approach, we first performed a test using three identical actuators simultaneously **(Fig. S34)**. Three hydrogel samples weighing about 2.6g, after sorption at 75% relative humidity, were simultaneously stimulated by three piezoelectric ultrasonic devices operating at a 25% duty cycle for 10-min. In all cases, the specimens exhibited a loss above 0.1 g. The measured specific energy consumption ranged from 1.9 to 2.1 MJ/kg after 2-min and from 4.2 to 5.8 MJ/kg after 10-min actuation (**Fig. S35**), comparable to the same values measured in a single-actuator device shown in **Table S4**.

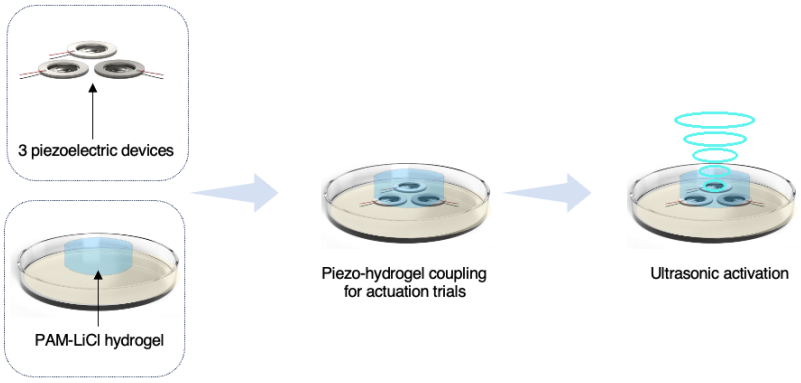

Figure S34: Desorption test of HG-A hydrogel specimens employing three individual piezoelectric ultrasound devices together.

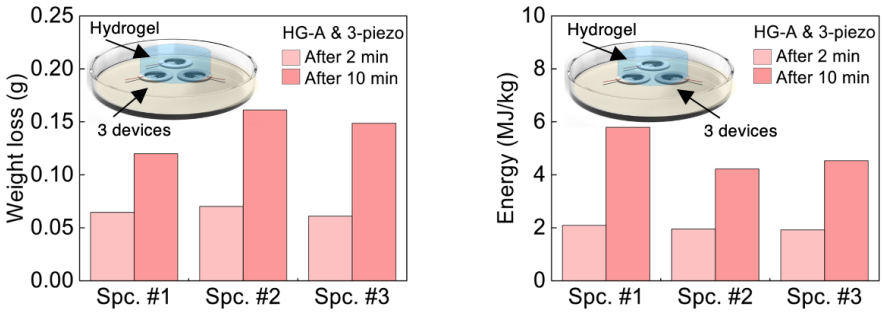

Figure S35: Desorption behaviour of HG-A hydrogel (~2.6 g per specimen) under the actuation of three individual piezoelectric ultrasound devices for 10 minutes at 25% duty cycle. The weight loss (left) and corresponding energy consumption (right) of the specimens (~2.6 g per specimen) after 2 and 10 min, respectively.

The daily yield of water from a 1-m^2 sorbent area [L/m^2/day] has been calculated by extrapolating the results of cyclic sorption-desorption testing of a single prototype device over 10 hours at 75% RH. The piezo actuator has a surface area of 0.0002 m^2 (diameter = 16mm), and the sorbent has a surface area of 0.0009 m^2 (diameter = 34 mm).

Fig. 6c shows the extracted water mass and energy efficiency for each extraction cycle (with ten 1-hour-long sorption cycles separated by eleven 2-minute-long extraction cycles). During each 2-minute-long extraction cycle, energy consumption was recorded to be below the enthalpy of water vaporization, thus yielding extraction efficiency in excess of 100%.

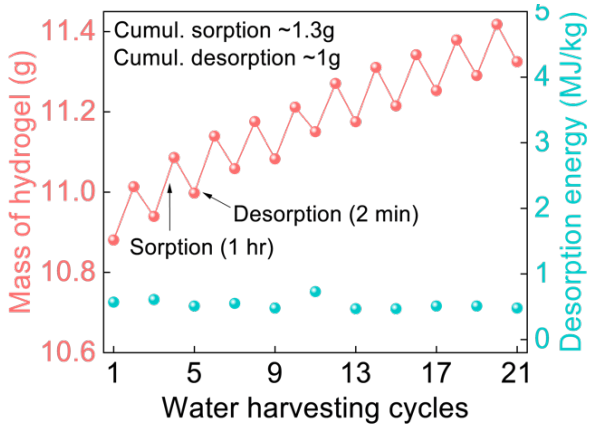

Figure 6c: Water sorption and desorption cycles of a large HG-A sorbent (>16 mm diameter) at 25% duty cycle.

To estimate the water yield per device per day, we first calculated the average sorption and desorption rates by using the data shown in **Fig. 6c and Fig. S36 (a)**. The average collection and extraction rate is around 0.13 g/hr and 0.08 g/2min **(Fig. 6c and S36a).** The extraction rate exceeds the collection rate by a factor of ~18.5, and during a 1-hr harvesting period, the sorbent collects more water than can be extracted in 2 min. These data indicate that to maximize and balance both the sorption and desorption processes over the course of one day, the system may be operated in 34 sorption-extraction cycles per 24 hours, each cycle comprised of about 40 minutes of collection followed by 2 minutes of extraction (see **Table S5**). Under this operational scenario, all the harvested moisture will be extracted with low energy expenditure, as it takes about 2 minutes to extract the whole amount of moisture harvested over 40 minutes at 75%RH. For operation at RH different than 75%, a different sorption-desorption cycle ratio may need to be implemented, to be optimized separately for each RH level.

To extrapolate the water yield to a 1-m^2 sorbent area, this number was further scaled up from one device having 0.0009-m^2 sorbent area to a 1-m^2-area array. The resulting average daily productivity value has been predicted to be ~3.2 [L/m^2/day]. Note that with our approach, harvesting can be done during both night and day (unlike the devices relying on solar-driven evaporation). In turn, the device efficiency of 0.16 kWh/kg (0.576 MJ/kg) was calculated by using the average mass extracted from each of two hydrogel specimens over eleven 2-min-long extraction cycles (see **Table S5**).

2.5. Supplementary Table 5. A summary of water harvesting cycles of larger HG-A (>16 mm diameter) sorbent.

	HG-A Specimen 1	HG-A Specimen 2	Average values
Collection per device per hour [g]	0.12	0.13	0.125
Collection per device per 40 minutes [g]	0.08	0.087	0.0835
Collection per device for 34 cycles [g]	2.77	2.96	2.865
Extraction per device per 2 min [g]	0.074	0.085	0.0795
Extraction per device for 34 cycles [g]	2.52	2.91	2.715
Collection per m^2 per day for 34 cycles [kg]	3.07	3.26	3.165
Extraction per m^2 per day for 34 cycles [kg]	2.77	3.19	2.98
Specific energy consumption [kWh/kg]	0.171	0.148	0.160

Fig. S36 (b) illustrates an alternative method of device operation, consisting of continuous harvesting for 24 hours at 75%RH, followed by desorption involving 25 consecutive cycles of 2-minute-long extractions over a total duration of 50 minutes (i.e., without a sorption period in between the cycles), resulting in the desorption of 1g of water at an energy cost of 1.13 MJ/kg. This energy expenditure is nearly a factor of two greater than the average energy cost observed for the 2-minute-long extraction cycles depicted in **Fig. S36 (a)**.

These methods together demonstrate the adaptability of our system, which is not constrained by temporal limitations, unlike the solar-derived desorption mechanism that operates based on the availability of sufficient or proper daylight hours at a slower desorption rate in comparison to our system. We chose the lower-energy-expenditure approach illustrated in **Fig. 6 (c)** to estimate the daily yield and the cost of the harvested water.

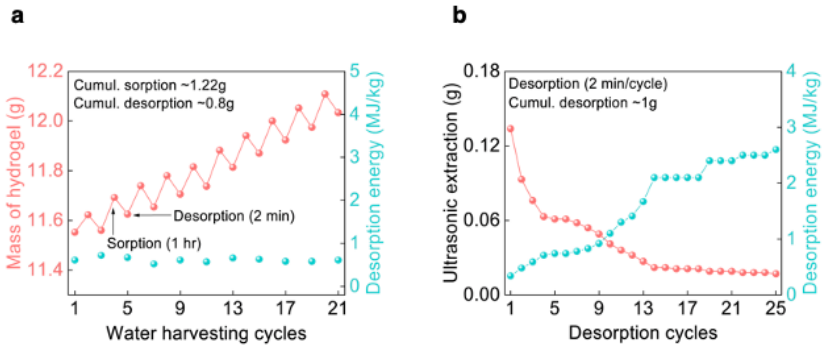

Figure S36: Two distinct strategies for water extraction from a sorbent: ten 1-hr sorption cycles separated by 2-min- extraction periods (a) and 25 cycles of subsequent 2-min extraction periods (b). This shows the stability, repeatability, and energy efficiency of the proposed system using

a large specimen (>16 mm diameter) for atmospheric water sorption and desorption with the energy consumption below the thermal limit.

We conducted similar studies with smaller specimens (≤16 mm diameter) and observed similar cyclic stability and energy efficiency as shown in **Fig. S37.** It can be seen that in this case the collection rate is much slower than the extraction rate, and during a 1-hr harvesting period, the sorbent collects less water than can be extracted in 2 minutes of actuation (see **Table S6**). As such, harvesting time imposes the upper limit on the daily water yield.

In this case, to balance the mass of harvested and extracted water over a 24-hour cycle, we assume 12 sorption-extraction cycles per 24 hours, each comprised of ~ 2 hours (118 min) of collection followed by ~2-minutes of extraction. During 118 min of collection, slightly less water is absorbed per device than can be extracted in 2 minutes, so we assume that each extraction period will be slightly less than 2 minutes long. The average daily water yield per device at 75%RH is calculated as the amount of water collected over twelve 118-min-long cycles. To extrapolate the water yield to a 1 m^2 sorbent area, this number was further scaled up from one device area to 1 m^2. The resulting average daily productivity value has been predicted to be ~1.5 [L/m^2/day], and the average energy consumption - 0.411 kWh/kg (1.48 MJ/kg).

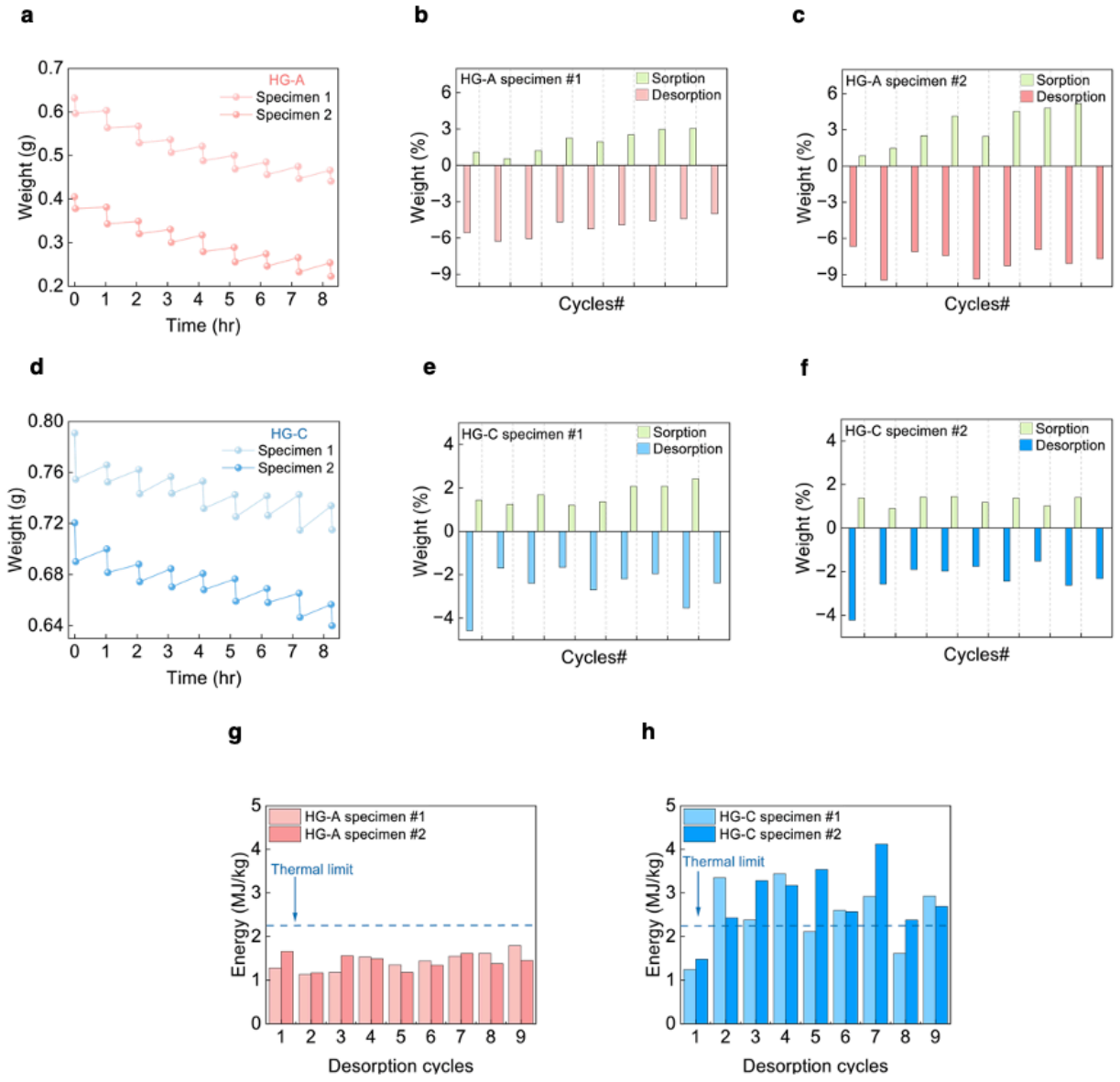

Figure S37: Stability, repeatability, and energy efficiency of the proposed system using smaller HG-A specimens (≤16 mm diameter) for atmospheric water sorption and desorption with the energy consumption below the enthalpy of water evaporation for both HG-A **(a-c, g)** and HG-C **(d-f, h).**

2.6. Supplementary Table 6. A summary of water harvesting cycles of smaller HG-A (≤16 mm diameter) sorbent.

	HG-A Specimen 1	HG-A Specimen 2	Average values
Collection per device per hour [g]	0.012	0.013	0.0127
Collection per device per 118 minutes [g]	0.024	0.026	0.025
Extraction per device per 2 minutes [g]	0.029	0.033	0.031
Collection per device per day [g]	0.289	0.31	0.3
Collection per m^2 per day [kg]	1.447	1.549	1.523
Specific energy consumption [kWh/kg]	0.426	0.396	0.411

1.6. Supplementary Note 6 – Structural integrity of hydrogel under ultrasonic extraction

To evaluate the structural integrity of the hydrogel and the extracted water quality after desorption, the water extracted from LiCl-PAM hydrogels (HG-A) were filtered using a VWR@ sterile syringe filter, commonly employed for ICP-OES testing. In this experiment, three piezoelectric devices were used to extract water from a ~5.92 g HG-A specimen at a duty cycle of 25-30% over a duration of ~45 min. The setup and test were made and conducted within an enclosed petri dish, respectively. Following desorption, ~0.21 ml of desorbed water was collected from the petri dish lid and subsequently filtered using a VWR filter paper kit to examine for any traces of polymer residue.

The initial dry weight of the filter paper kit was ~2.99 g, which increased to ~3.02 g after the filtration of ~0.21 ml extracted water at 20% relative humidity, resulting in wetting the filter paper. Following drying at room temperature, the weight of the filter paper returned to 2.99 g, with no polymer residue detected. This provides the evidence that hydrogels remained intact following the ultrasonic actuation process, and the extracted water is not contaminated by the polymer.

1.7. Supplementary Note 7 – Li content in the water extracted from LiCl-PAM hydrogels

We additionally analyzed Li content in the water extracted from LiCl-PAM hydrogels. There are no regulatory thresholds for lithium either in the USA or globally, and EPA doesn't have a specific health advisory for lithium in a drinking water [15,16]. While typical therapeutic oral doses of Li are as high as 600–1200 mg/day [17], Li may pose a potential concern for human health, and some studies recommend to limit casual Li-ion intake to 3.1 mg per day[18]. At the same time, recent studies of of bottled water from dozens of countries revealed a wide range of Li content, from ~0 to 9.9 mg/L [16,19].

We conducted the inductively coupled plasma optical emission spectrometer (ICP-OES) elemental analysis on the water desorbed from a LiCl-PAM hydrogel to test its quality**.** The resultant Li-ion concentration varied between 1.5 and 15.2 ppm (or mg/L), see **Supplementary Fig. S38**. However, the presence of Li ions plays no role in the energy efficiency of water extraction, and our work demonstrates that our methodology is equally applicable to Li-free hydrogels such as HG-M. Our future work will focus on the synthesis and testing of Li-free sorbents with high water uptake to limit the risk of water contamination and to reduce the cost of the technology.

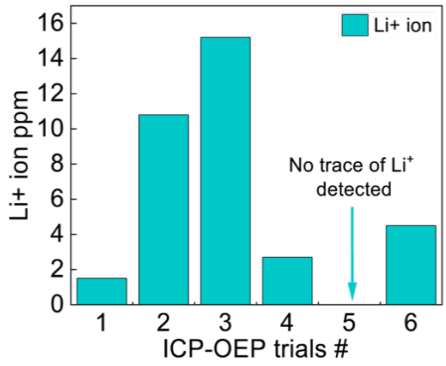

Figure S38: Inductively coupled plasma optical emission spectrometry (ICP-OES) elemental analysis of the lithium-ion content in extracted water after sorption at 20% RH.

1.8. Supplementary Note 8 – Contributions of mechanical actuation and heating of the device

By modifying the technoeconomic feasibility study conducted by Zhong et al.[10] on sorption-based atmospheric water harvesting (SAWH) system, we carried out a preliminary technoeconomic analysis of our system. Contrary to that study, we consider that the lifespan of the material and device are distinct. In addition, we included the cost of supplied electric power into cost of water production (Cost of water, in units of $/L), which is calculated as:

$$\text{Cost of water} = \text{Capital expenditure (CAPEX)} + \text{Operational expenditure (OPEX)}$$

$$= \frac{\left(\frac{(\text{Cost}_{\text{hydrogel}} \cdot \rho_{\text{hydrogel}} \cdot V_{\text{hydrogel}}}{\tau_{\text{hydrogel}}} + \frac{\text{Cost}_{\text{device}}}{\tau_{\text{device}}}\right)}{\text{Yield}} + (\text{Electricity cost} \cdot \text{Energy intensity})$$

(Eqn. S11)

Here,

$\text{Cost}_{\text{hydrogel}}$ = cost of hydrogel-salt composite per kg of material in the dry state,

ρ_{hydrogel} = density (2000 kg/m^3)[20] of the hydrogel-salt composite in the dry state,

$V_{\text{hydrogel}} = A_{\text{hydrogel}} \cdot H_{\text{hydrogel}}$ = volume of the hydrogel-salt composite in the dry state,

A_{hydrogel} = 1 m^2 area of the hydrogel-salt composite, making cost per m^2 of our overall system,

H_{hydrogel} = typical hydrogel-salt composite thicknesses used in our device ~1mm (=0.001m),

τ_{hydrogel} = hydrogel lifetime in days (30-365 days), which is one of the variables of analysis,

$\mathrm{Cost}_{\mathrm{device}}$ = cost of the SAWH device excluding the sorbent cost,

τ_{device} = lifetime of the piezoelectric PZT actuator (20-45 years), which is another variable [21,22],

Yield or productivity = amount of water produced by day (L/m^2/day),

Electricity cost = 0.17 \$/kWh, electricity price based on US Bureau of Labor Statistics [23],

Energy intensity = supplied energy per liter of desorbed water, expressed in kWh/L

Table S7 summarizes all the costs of the hydrogel-salt composite ingredients and an actuator unit as well as the energy cost of operating the actuator. With these data, we estimate the $\mathrm{Cost}_{\mathrm{hydrogel}}$ and $\mathrm{Cost}_{\mathrm{device}}$ are 0.4-1.1 \$/kg and 1111-2222 \$/m^2 (based on a single device used for a gel with 34 mm diameter), respectively.

2.7. Supplementary Table 7. Parameters used in estimating the cost of water production.

Component	Amount used	Price	Ref.
Lithium chloride *	0.8 kg	0.1-1 \$/kg	24
Acrylamide	0.2 kg	1.6 \$/kg	25
Ammonium persulfate	0.68 g	0.61 \$/kg	26
N,N'-methylenebisacrylamide	2.4 g	1 \$/kg	27
N,N,N′,N′-tetramethylethylendiamin	0.57 mL or 0.44 g [28]	10 \$/kg	29
Ultrasonic system *	1 unit	1-2 \$/unit	30
Electricity cost **	0.00025 kWh	0.0002 \$/10min	31

* The price fluctuated during the study duration

** Estimated for a single unit

The daily yield of water of 3.2 kg/m^2/day has been estimated from the results of the cyclic sorption/extraction experiment as detailed in **Supplementary note 5** above. CAPEX, OPEX, and cost of water were then estimated to be 0.05-0.09 \$/L, 0.1 \$/L, and 0.19 \$/L **(Fig. S39**) assuming the device lifespan of 25 years and hydrogel lifespan of 30 days **(Fig. S40**). Based on a worldwide survey conducted on 2023, the cost of a fresh bottled water, ranges between 0.23 and 1.35 \$/L around the globe as shown in **Fig. S39,** and thereby, estimated to have an average price of 0.79 \$/L **(**data taken from [32]**).**

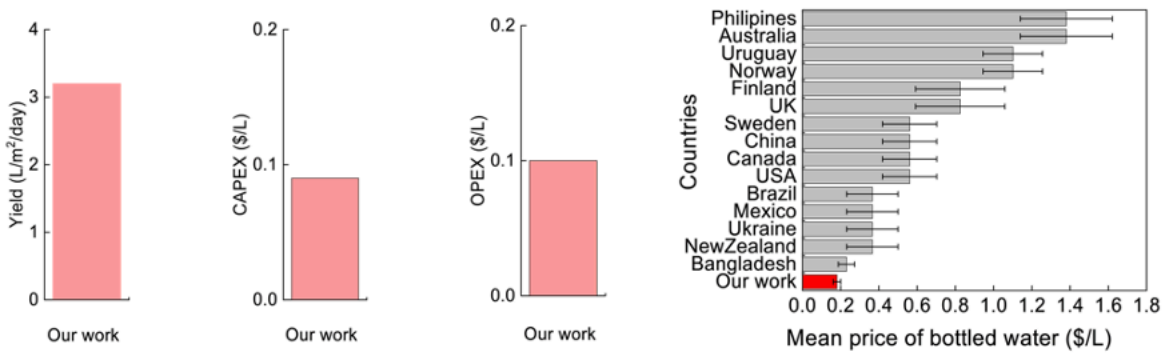

Figure S39: A summary of the parameters (productivity, OPEX, and CAPEX) used in our techno-economic analysis to estimate the price of water ($/L) and a comparative study of mean price of bottled water among the countries.

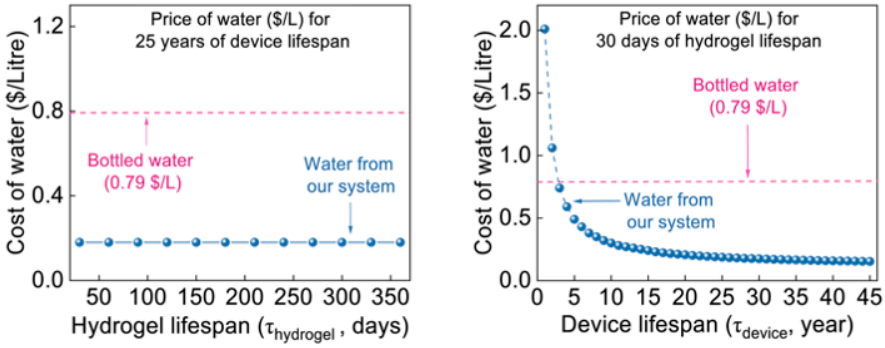

Figure S40: Estimated cost of water as a function of hydrogel **(a)** and device **(b)** lifetime.

1.9. Supplementary Note 9 – Contributions of mechanical actuation and heating of the device

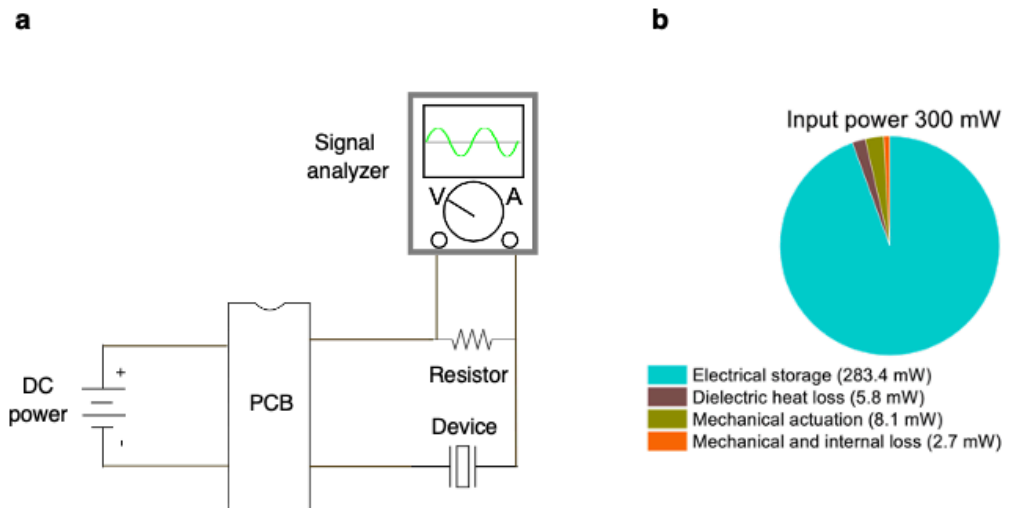

Figure S41. Circuit diagram **(a)** used to characterize the input power fed to the piezoelectric transducer and a rough estimate of the power breakdown spent on thermal and mechanical actuation (**b**).

With the hardware configuration shown in the circuit diagram in **Fig. S41 (a),** we measured that approximately 300 mW of the supplied 1.5W DC power enters the piezoelectric ultrasound device. Based on our estimated effective coupling coefficient for the PZT device, the actuator efficiency (η_a) — that is, the ratio of electrical energy consumed to the mechanical energy produced — is $\eta_a = k_{eff}^2 = 3.6\%$. In the case of perfect coupling (i.e., $\eta_a = 100\%$), the mechanical loss tangent, $\tan\varphi$, would have been $1/Q = 1/32 = 3.1\%$ (where Q is the quality factor of PZT-5H ceramic), and 3.1% of the input power would be lost as heat[33,34]. Since the actual coupling efficiency is only 3.6%, the actual heat losses are 3.1% of 3.6% plus another portion of the 3.6% associated with work done by the PZT. We assume that the combination of the work done on the hydrogel by the PZT system during its contraction and expansion and the internal mechanical losses of the PZT material itself comprise roughly 25% of the mechanical energy, which is lost as heat, i.e., 25% of 3.6% (i.e., 0.9% of 300 = 2.7 mW). The remaining energy is attributed to mechanical storage, calculated as 2.7% (=3.6% - 0.9%) of 300 mW, which is equal to 8.1 mW.

As piezoelectric devices are essentially capacitors, the bulk of the delivered electrical energy is stored energy, which ultimately returns to the power source. The power delivered to the piezoelectric capacitor is about 96.4% (=100% - 3.6%) of the 300 mW input power, which is 291 mW. The dielectric loss tangent, $\tan\delta_e$, for PZT-5H piezoelectric ceramics is about 2%, and the lost power is dissipated as heat, generating about 5.8mW, i.e., 2% of 291 mW. Hence, the combined mechanical and dielectric power loss to heat is therefore about $5.8\ mW + 2.7\ mW = 8.5\ mW$ when the actuator is driven at its resonant frequency.

In summary, we estimate the energy consumption to be roughly equally divided between the mechanical actuation and heating, with individual contributions measuring 8.1 mW (49%) and 8.5

mW (51%), respectively, while 283.4 mW were returned to the power source (**Fig. S41b)**. Due to the complexity of quantifying the dynamic interaction between the ceramic, the metallic membrane, and the hydrogel during actuation we offer this relatively simplistic analysis to quantify the individual contributions of work, mechanical losses, and dielectric losses. Future work will aim to develop a more comprehensive model to decouple the different effects of heat and vibration on different actuators and sorbents.

References:

1. LaPotin, A., Zhong, Y., Zhang, L., Zhao, L., Leroy, A., Kim, H., Rao, S. R. & Wang, E. N. Dual-Stage Atmospheric Water Harvesting Device for Scalable Solar-Driven Water Production. *Joule* **5,** 166–182 (2021).
2. Li, S., Xu, J., Li, R., Wang, Y., Zhang, M., Li, J., Yin, S., Liu, G., Zhang, L., Li, B., Gu, Q. & Su, Y. Stretchable Electronic Facial Masks for Sonophoresis. *ACS Nano* **16,** 5961–5974 (2022).
3. Polmar, N. The U.S. Navy: Tails for Warships. *Ships Aircr. U. S. Fleet* (1987). at <https://www.usni.org/magazines/proceedings/1987/october/us-navy-tails-warships>
4. Dupuis, E. D., Momen, A. M., Patel, V. K. & Shahab, S. Electroelastic investigation of drying rate in the direct contact ultrasonic fabric dewatering process. *Appl. Energy* **235,** 451–462 (2019).
5. Zhu, X., Zhang, Z., Hinds, L. M., Sun, D.-W. & Tiwari, B. K. Applications of ultrasound to enhance fluidized bed drying of Ascophyllum Nodosum: Drying kinetics and product quality assessment. *Ultrason. Sonochem.* **70,** 105298 (2021).
6. Daghooghi-Mobarakeh, H., Campbell, N., Bertrand, W. K., Kumar, P. G., Tiwari, S., Wang, L., Wang, R., Miner, M. & Phelan, P. E. Ultrasound-assisted regeneration of zeolite/water adsorption pair. *Ultrason. Sonochem.* **64,** 105042 (2020).
7. Lu, H., Shi, W., Zhang, J. H., Chen, A. C., Guan, W., Lei, C., Greer, J. R., Boriskina, S. V. & Yu, G. Tailoring the Desorption Behavior of Hygroscopic Gels for Atmospheric Water Harvesting in Arid Climates. *Adv. Mater.* **34,** (2022).
8. Graeber, G., Díaz-Marín, C. D., Gaugler, L. C., Zhong, Y., El Fil, B., Liu, X. & Wang, E. N. Extreme Water Uptake of Hygroscopic Hydrogels through Maximized Swelling-Induced Salt Loading. *Adv. Mater.* **2211783,** 1–10 (2023).
9. Wilson, C. T., Cha, H., Zhong, Y., Li, A. C., Lin, E. & El Fil, B. Design considerations for next-generation sorbent-based atmospheric water-harvesting devices. *Device* **1,** 100052 (2023).
10. Zhong, Y., Zhang, L., Li, X., El Fil, B., Díaz-Marín, C. D., Li, A. C., Liu, X., LaPotin, A. & Wang, E. N. Bridging materials innovations to sorption-based atmospheric water harvesting devices. *Nat. Rev. Mater.* **9,** 681–698 (2024).
11. Hanikel, N., Prévot, M. S., Fathieh, F., Kapustin, E. A., Lyu, H., Wang, H., Diercks, N. J., Glover, T. G. & Yaghi, O. M. Rapid Cycling and Exceptional Yield in a Metal-Organic Framework Water Harvester. *ACS Cent. Sci.* **5,** 1699–1706 (2019).
12. Xu, J., Li, T., Yan, T., Wu, S., Wu, M., Chao, J., Huo, X., Wang, P. & Wang, R. Ultrahigh solar-driven atmospheric water production enabled by scalable rapid-cycling water harvester with vertically aligned nanocomposite sorbent. *Energy Environ. Sci.* **14,** 5979–5994 (2021).

13. Shan, H., Li, C., Chen, Z., Ying, W., Poredoš, P., Ye, Z., Pan, Q., Wang, J. & Wang, R. Exceptional water production yield enabled by batch-processed portable water harvester in semi-arid climate. *Nat. Commun.* **13,** 5406 (2022).
14. Almassad, H. A., Abaza, R. I., Siwwan, L., Al-Maythalony, B. & Cordova, K. E. Environmentally adaptive MOF-based device enables continuous self-optimizing atmospheric water harvesting. *Nat. Commun.* **13,** 4873 (2022).
15. Adeel, M., Zain, M., Shakoor, N., Ahmad, M. A., Azeem, I., Aziz, M. A., Tulcan, R. X. S., Rathore, A., Tahir, M., Horton, R., Xu, M. & Yukui, R. Global navigation of Lithium in water bodies and emerging human health crisis. *npj Clean Water* **6,** 33 (2023).
16. Iordache, A. M., Voica, C., Roba, C. & Nechita, C. Lithium Content and Its Nutritional Beneficence, Dietary Intake, and Impact on Human Health in Edibles from the Romanian Market. *Foods* **13,** 592 (2024).
17. Szklarska, D. & Rzymski, P. Is Lithium a Micronutrient? From Biological Activity and Epidemiological Observation to Food Fortification. *Biol. Trace Elem. Res.* **189,** 18–27 (2019).
18. Schrauzer, G. N. Lithium: Occurrence, Dietary Intakes, Nutritional Essentiality. *J. Am. Coll. Nutr.* **21,** 14–21 (2002).
19. KRACHLER, M. & SHOTYK, W. Trace and ultratrace metals in bottled waters: Survey of sources worldwide and comparison with refillable metal bottles. *Sci. Total Environ.* **407,** 1089–1096 (2009).
20. Conde, M. R. Properties of aqueous solutions of lithium and calcium chlorides: formulations for use in air conditioning equipment design. *Int. J. Therm. Sci.* **43,** 367–382 (2004).
21. Moussa, R. R. The Effect of Piezo-Bumps on Energy Generation and Reduction of the Global Carbon Emissions. in *WSEAS Trans. Environ. Dev.* (WSEAS, 2019). at <https://wseas.com/journals/articles.php?id=1976>
22. PI Ceramic. *Reliability & Lifetime of Multilayer Piezo Actuators*. (2025). at <https://www.pi-usa.us/fileadmin/user_upload/pi_us/files/catalogs/Piezo_Actuator_Lifetime_Test_Reliability_Results.pdf>
23. US Bureau of Labor Statistics. Average Energy Prices, Boston-Cambridge-Newton — December 2024. *News Release* (2024). at <https://www.bls.gov/regions/northeast/news-release/averageenergyprices_boston.htm>
24. High Purity Lithium Chloride 99% Cas 7447-41-8 - Buy Lithium Chloride cas 7447-41-8 welding Agent Product on Alibaba.com. *Alibaba.com* (2024). at <https://www.alibaba.com/product-detail/High-Purity-Lithium-Chloride-99-CAS_1600991631465.html>
25. Shandong Up Chemical Technology. China Factory Price Acrylamide 98%Acrylamide. *Alibaba.com* (2024). at <https://www.alibaba.com/product-detail/China-factory-price-Acrylamide-98-Acrylamide_1600137018371.html>
26. Nanjing Jiayi Sunway Chemical Ltd. Ammonium Persulfate (NH4)2S2O8 CAS 7727-54-0 Ammonium Persulfate 98.66%. *Alibaba.com* (2024). at <https://www.alibaba.com/product-detail/Ammonium-Persulfate-NH4-2S2O8-CAS-7727_1601015455421.html>
27. Qingdao Jinyu Chemical. NN-Methylenebisacrylamide MBA Methylene Bisacrylamide CAS 110-26-9. *Alibaba.com* (2024). at <https://www.alibaba.com/product-detail/factory-

direct-supply-N-N-Methylenebisacrylamide_1600882499349.html>
28. Sigma. N,N,N′,N′-Tetramethylethylenediamine (≥99.5%, purified by redistillation). *Sigma-Aldrich Chem. Build. Blocks* (2024). at <https://www.sigmaaldrich.com/US/en/product/aldrich/411019>
29. N,N,N',N'-tetramethylethylenediamine With Low Price Cas 110-18-9 - Buy Tmeda,Cas 110-18-9 Tmeda. *Alibaba.com* (2024). at <https://www.alibaba.com/product-detail/N-N-N-N-Tetramethylethylenediamine-with_1600272967916.html>
30. Dongguan Cosson Electronic Plastic Ltd. 16mm Ultrasonic Mist Maker with Small Driver Circuit. *Alibaba.com* (2025). at <https://www.alibaba.com/product-detail/16mm-Ultrasonic-Mist-Maker-with-Small_60392165208.html?spm=a2700.details.you_may_like.1.7b8f2d7fBLILGw>
31. U.S. Energy Information Administration. Average Price of Electricity to Ultimate Customers. *Electr. Power Mon.* (2025). at <https://www.eia.gov/electricity/monthly/epm_table_grapher.php?t=epmt_5_3>
32. Statista. How Much Does a Bottle of Water Cost? *Bottled water Mark. Worldw.* (2023).
33. Bilgen, O., Amin Karami, M., Inman, D. J. & Friswell, M. I. The actuation characterization of cantilevered unimorph beams with single crystal piezoelectric materials. *Smart Mater. Struct.* **20,** 055024 (2011).
34. Fuji Ceramics. PZT Material Selection Guide. *Fuji Ceram. Corp.* (2022). at <https://www.fujicera.co.jp/en/feature/4164/>

Response to the reviewers for the manuscript:

High-efficiency atmospheric water harvesting enabled by ultrasonic extraction

by

Ikra Shuvo[1], Carlos D. Díaz-Marín[2], Marvin Christen[4], Michael Lherbette[4], Christopher Liem[3], Svetlana V. Boriskina[2]*

[1]*Media Lab, Massachusetts Institute of Technology, Cambridge, MA 02139, USA*

[2]*Department of Mechanical Engineering, Massachusetts Institute of Technology, Cambridge, MA 02139, USA*

[3]*Department of Electrical Engineering and Computer Science, Massachusetts Institute of Technology, Cambridge, MA 02139, USA*

[4]*SmarAct Metrology GmbH & Co. KG, Oldenburg, HRA 207391, Germany.*

*Corresponding author: sborisk@mit.edu

We are grateful for the constructive comments from the reviewer on our manuscript. The reviewer's comments are in blue, with our responses for each specific comment below. The text that has been added to the revised manuscript is colored red. To properly address the comments from Reviewer #4, we added several new Supplementary Notes to the revised version of the manuscript. These notes are included in this letter and are referenced in our responses below.

Reviewer #4:

I have carefully reviewed the manuscript by Shuvo and Boriskina et al. before considering the comments and suggestions raised by the other reviewers in the previous review cycle. This work does report an interesting phenomenon in the field of atmospheric water harvesting (AWH) that water can be extracted from a hydrogel by using an ultrasonic actuator. The authors convincingly demonstrated that they are attempting to address one of the major challenges in the field: the optimization of energy consumption for sorbent regeneration and freshwater production. However, I also have similar concerns to other reviewers in terms of energy consumption and calculations, water qualities, scalabilities, etc., even though with the resubmitted manuscript.

(1) It is known that the thermally-driven sorbent regeneration and freshwater production systems can make direct use of low-grade energy, such as waste heat, or thermal energy converted from solar energy. The ultrasonic water extraction reported in this work relies entirely on electricity, a

high-grade secondary energy and substantial energy losses occur during electricity generation. For example, commercial PV modules normally converts only ~15-20% of incident energy in practice while thermal power plant converts approximately 30-40% of energy from burning fossil fuels. If these upstream losses are counted, the ultrasonic route suffers a three- to five- fold increases in primary energy demand and a correspondingly larger carbon footprint.

We thank the reviewer for raising this important point. Indeed, thermal power plants convert approximately 30-40% of energy from burning fossil fuels, because they operate at high temperatures. In contrast, the efficiency of solar-thermal energy conversion is typically much lower because of energy loss through thermal re-radiation and entropy generation during the photon absorption-emission process[1–3]. The efficiency can be increased by increasing operating temperatures, which however requires the use of solar concentrators and highly frequency-selective absorbers. Not only this increases the installation capital costs, but also such high temperatures may damage the sorbents and create local heat islands around the AWH devices. We have included a new **Supplementary Note 11**, which discusses in detail the origin of the low efficiency of the solar-thermal energy conversion process.

There are additional arguments for the use of a PV cell to convert and store solar energy to power an outdoor AWH system (even if ultrasonic extraction is not used). The daily water yield per land area can be maximized by designing vertically-oriented systems[4,5] integrated with ultrasonic actuators (or PV-powered Joule heaters) for extraction, and by optimizing the sorption-desorption cycle duration to operate around the clock. Other auxiliary devices can be powered by the PV-generated electricity, including sensors to monitor environmental conditions and fans to promote air convection to improve vapor diffusion[4,6]. Finally, AWH systems with vibrational extraction can be designed to run autonomously, avoiding manual batch-drying process[7] and adapting their sorption/extraction cycles to varying environmental conditions.

The above paragraph has been added to the Discussion section of the revised manuscript.

1.10 Supplementary note 11

This note discusses the efficiency of the process of solar-thermal energy conversion. **Supplementary Fig. S40a** illustrates a schematic of a solar absorber modeled as an ideal thermal engine. The energy is delivered to the engine via solar radiation and the entropy is transferred to the environmental heat sink via heat conduction. The absorber heats up to a steady-state temperature T_A and emits photons back to the environment in the form of incoherent thermal radiation. A general expression for the efficiency of this engine takes the following form:

$$\eta_{S-T} = \frac{W}{I_S} = \frac{1}{I_S}\left(I_S - \left[I_A(T_A) + T_a\left[S_S(T_S) - S_A(T_A) + S_g\right]\right]\right)$$

Here, I_S and S_S are the solar energy flux and the corresponding entropy flux, respectively. $T_S = 5779\ K$ is the Sun's effective emission temperature. T_A is the temperature of the solar absorber

emitting energy flux I_A and the corresponding entropy flux S_A. For the blackbody thermal emission process, $I_A = \sigma T_A^4$ and $S_A = \frac{4}{3}\sigma T_A^3$, where σ is the Boltzmann constant.

The entropy flux of thermal radiation S_A is calculated via integration over photon energy and direction of light propagation, and deviates from the conventional definition of the entropy for thermal processes driven by heat conduction, which would result in the expression $S = \frac{I}{T} = \sigma T^3$. While the Sun is a blackbody, angular and spectral filtering of solar radiation arriving to the Earth surface reduces its entropy dramatically, to $S_S = \frac{4}{3}\frac{\Omega_0 \cos\theta_0}{\pi}\sigma T_S^3$, where the global averaged cosine of solar zenith angle $\cos\theta_0$ is 0.25, and the solar solid angle is $\Omega_0 = 6.77 \cdot 10^{-5}$ sr.

Entropy generated in the process of solar energy absorption in a blackbody absorber and partial re-emission back to the environment in the form of thermal emission can be calculated as follows:

$$S_g = I_S\left(\frac{1}{T_A} - \frac{4}{3}\frac{1}{T_S}\right) + \frac{1}{3}\frac{I_A}{T_A}$$

This combination of energy loss through thermal re-radiation and entropy generation during the photon absorption-emission process significantly restricts the maximum efficiency of the solar-thermal energy conversion. For comparison, I_S can reach 1,000 W/m² on a clear day at solar noon and is lower in the presence of clouds or during early/late hours of the day. In turn, the energy flux emitted by a blackbody absorber at 60°C (which is a typical temperature used for sorbent regeneration) is approximately 687.6 W/m². As a result, the solar-thermal energy conversion efficiency reaches a limit of only ~15% for a blackbody absorber illuminated by sunlight without concentrating optics (i.e., under one sun illumination)[1,2], see **Supplementary Fig. S40b**.

Solar concentration using external lenses or reflectors can increase the absorber temperature by focusing sunlight and increasing the solar energy flux per surface area (**Supplementary Fig. S40c)**. This results in the increased efficiency of soler-thermal energy conversion (**Supplementary Fig. S40b)**, but requires installation of additional components, such as solar concentrators and trackers, increasing the system cost and footprint.

To suppress re-emission losses, solar absorbers with a stepwise emittance spectrum can be engineered[8–12], which exhibit high absorptance across most of the solar spectrum, and zero emittance at lower frequencies overlapping with the thermal emission spectra. As illustrated in **Supplementary Figs. S40b,c**, an absorber with 90% solar absorptance and 10% infrared emittance can increase the maximum possible efficiency of the solar energy conversion. Note that due to the presence of atmospheric absorption bands in the solar spectrum, the equilibrium temperature does not vary smoothly with the solar concentration, as evidenced by the kinks in **Supplementary Fig. S40**c[13]. However, water has very high infrared emittance[14], making this strategy inapplicable to engineering AWH sorbents.

For comparison, as illustrated in **Supplementary Fig. S40a**, the PV conversion efficiency of solar energy to electricity reaches about 20-25% for a single-junction commercial PV cell under 1-sun unconcentrated sunlight illumination[15–19]. It can be further increased if multiple-junction PV cells

are used under concentrated sunlight, and the energy can be either used immediately or stored for use during nighttime.

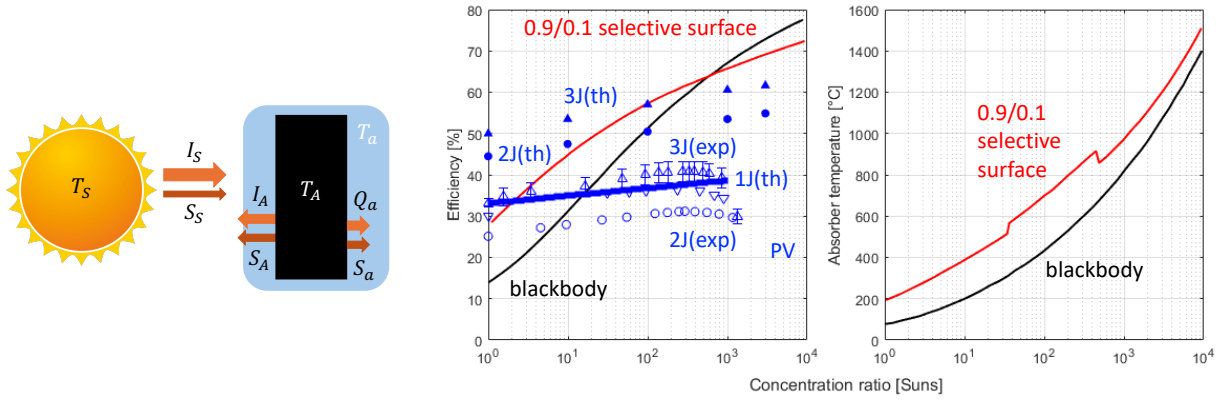

(a) (b) (c)

Supplementary Figure S40. (a) A schematic of a solar-thermal energy converter with the energy and entropy fluxes illustrated. **(b)** The limiting efficiency of solar thermal energy converters with a blackbody (black solid line) and a spectrally selective (red solid line) absorber as a function of solar concentration. The converted are assumed to operate at the Carnot efficiency. For spectrally selective absorbers, the transition frequency between high and low solar/infrared emittance levels (labeled as ratios α/ε) is optimized for each concentration ratio[1]. **b.** The corresponding equilibrium temperature of the solar-thermal absorbers with the optimized spectral transition point between high and low emittance levels as a function of solar concentration. Blue markers on panel (a) represent energy efficiency of PV cells [15–19]. Solid markers represent theoretical predictions (squares: a single-junction cell, circles: a dual-junction cell, triangles: a triple junction cell). Hollow markers correspond to the experimental data (circles: dual-junction, triangles: triple junction cells).

(2) The daily freshwater yield of the ultrasonic approach is projected at around 3.2 L m^{-2} day^{-1}; by contrast, the state-of-the-art solar-thermal systems already deliver much higher productivity, for example, 3.65 L/m2/day (Energy Environ. Sci., 2024, 17, 4988-5001), 3.5-8.9 L/m2/day (Nat. Commun. 2024, 15, 7678), 5.02 L/m2/day (Adv. Funct. Mater. 2025, 2501163), etc., by using only solar energy. It is premature to conclude that ultrasonic-driven process outperforms its thermal-based counterparts.

The daily yield of any AWH system is limited by both the sorption and desorption rates. Our research shows that by using ultrasound desorption mechanism, the total daily yield is almost entirely constrained by the sorption rate of the used sorbent. The well-studied PAM-LiCl hydrogel used in this work adsorbs the same amount of moisture from air with 75% RH in 40 minutes as can be extracted by piezo actuation in 2 minutes.

The daily yield value of 3.25 L m^{-2} day^{-1} was [very conservatively] estimated under these assumptions:

- multiple identical actuators with hydrogel samples identical to those used in our study are deployed in the form of a 2D horizontal array with the total area of the sample surface equal to 1 m^2
- each actuator is powered separately and the energy consumption per device is the same as measured in our experiments

It should be emphasized that ultrasonic extraction does not require exposing sorbent surface to sunlight. Accordingly, AWH devices can be stacked vertically on top of each other with no limitation in principle to the number of vertical rows. Adding more 2D device arrays by stacking them vertically will increase the yield by 3.25 L day^{-1} per each row without increasing the installation horizontal footprint. For instance, using an installation with 5 vertical rows of devices, the productivity of our system can be increased fivefold to 16.25 L day^{-1} per m^2 of horizontal footprint. **Figure 6d** and **Supplementary Table 7** compare the estimated productivity of our system with those of previously reported AWH materials and systems. Replacing PAM-LiCl hydrogels with sorbents exhibiting higher sorption rate (such as e.g. a hygroscopic interconnected porous gel[4]) can further increase daily yield.

Vertical stacking or vertical arrangement of sorbents have already been used in the state-of-the-art AWH systems with thermal extraction to increase per-m^2 yield[4,5,20,21]. However, except for the vertically oriented sorbent setup employing integrated Joule heaters[5], such installations require either manual batch processing of sorbent layers, or conveyor-belt-like rotating sorbents to achieve solar exposure for thermal extraction.

We included the above two paragraphs to the discussion section and added a new panel to Figure 6 (**Fig. 6d**) to compare the estimated productivity of our system to the state-of-the art results (both, in units of L m^{-2} day^{-1} and L kg^{-1} day^{-1}). The data plotted in **Fig. 6d** are summarized in a new **Supplementary Table 7**.

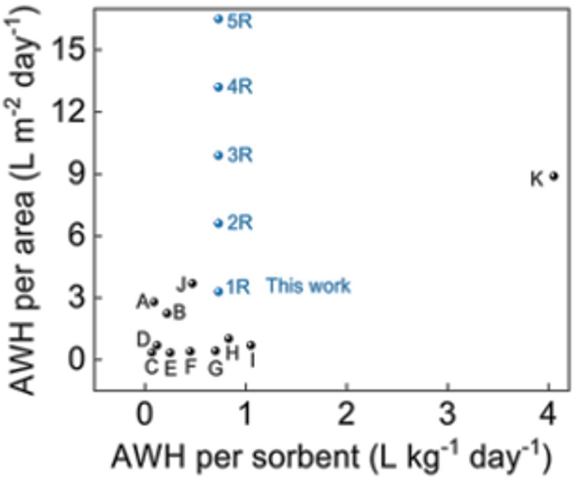

Figure 6d: Predicted water productivity compared to the results of prior studies (sorbent layers stacked vertically in multiple rows with a 1 m^2 horizontal footprint).

2.7. Supplementary Table 7. Comparison of water productivity among different studies.

Sl	RH%	AWH per sorbent (L kg^{-1} day^{-1})	AWH per area (L m^{-2} day^{-1})	Reference	Water harvesting configuration
A	80	0.09	2.8	[22]	Single rectangular liquid sorbent bed of [EMIM][Ac]
B	70-90	0.22	2.25	[23]	Rolled-up 4-pcs of ACF-$CaCl_2$ sorbent bed
C	<20	0.07	0.35	[24]	Single MOF-801 sorbent bed
D	57-68	0.12	0.7	[25]	Vertically stacked 2-pcs of AQSOA Z01 zeolite bed
E	10-40	0.25	0.34	[26]	Single rectangular MOF-801 sorbent bed
F	30	0.45	0.4	[27]	Single circular pot of LiCl@MIL-101(Cr)
G	10	0.7	0.43	[28]	A modular MOF-303 exchanger cartridge
H	60	0.83	1.02	[29]	A rotational cylinder loaded with LiCl capsule sorbent
I	40-70	1.05	0.7	[30]	Batchwise continuous production using a sorbent bed made of LiCl@rGO–SA
J	50	0.47	3.7	[20]	Vertically organized 5 sorbent beds made of LiCl@rGO–SA working in batches
K	57	4.05	8.9	[31]	Vertically rotatable sorbent bed made of salt-based HIPG powered by wind at >1 m/s
1R	75	0.73	3.25	This work	One 1-m^2-area row of devices
2R	75	0.73	6.5	This work	Two 1-m^2-area rows of devices
3R	75	0.73	9.75	This work	Three 1-m^2-area rows of devices
4R	75	0.73	13.0	This work	Four 1-m^2-area rows of devices
5R	75	0.73	16.25	This work	Five 1-m^2-area rows of devices

(3) Another critical question is whether AWH remains advantageous when scaled to grid-connected systems. At a relative humidity of 75 %, a level the experiment of this work carried out for freshwater productivity prediction, AWH can indeed produce water. However, the availability of grid electricity removes the energy constraint that AWH is designed to circumvent. Under such conditions, conventional condensation technologies (e.g., dehumidifiers) are likely to deliver significantly higher water yields and should be evaluated as the more favorable option than the ultrasonic approach.

Conventional condensation technologies use a dewing process, which cools air to its dewing point and then condenses it. At $\omega_0 = 75\%$ RH and $T_0 = 25°C$, the minimum energy required for the ideal dewing process is 0.58 MJ/kg (0.16 kWh/kg), see a new **Supplementary Note 6** below.

Our work yielded an experimentally measured device-level energy intensity as low as 0.324 MJ/kg (0.09 kWh/kg, first cycle in **Fig. 6b)**, with an average over multiple cycles of 0.15 kWh/kg at 75% RH, **Fig. 6a**.

On a separate note, even small-scale dehumidifiers produce a lot of noise [32].

1.6 Supplementary Note 6 – Ideal limit of moisture extraction from air by dewing

The minimum energy intensity per unit mass of water $\frac{Q_{in}}{m_w}$ required for dewing can be calculated as follows:

$$\frac{Q_{in}}{m_w} = \left[\frac{1}{\omega_i}(c_{p,air} + \omega_0 c_{p,v})(T_0 - T_r) + h_{fg}\right] COP^{-1},$$

where ω_0 is the ambient humidity, $c_{p,air}$ and $c_{p,v}$ are the specific heat capacity of air and vapor, respectively, T_r is the dewpoint temperature, and h_{fg} is the enthalpy of vaporization of water at T_0, equivalent to the latent heat removed during condensation. The term $\frac{1}{\omega_i}(c_{p,air} + \omega_i c_{p,v})(T_0 - T_r)$ represents the sensible heat removed from the air and moisture to cool it down to the dew point temperature. COP is the coefficient of performance of the refrigerator used to remove heat. For an ideal refrigerator, $COP = \frac{T_r}{T_0 - T_r}$.

At $\omega_0 = 75\%$ RH and $T_0 = 25°C$, the minimum energy required for dewing is 0.58 MJ/kg (0.16 kWh/kg). This is an ideal limit (corresponding to $COP = 4.32$).

Actual dehumidifying systems typically operate at COP values between 3 and 4, which will increase the energy intensity to 0.23 kWh/kg or 0.173kWh/kg, respectively. As an example, whole-home dehumidifiers with a volume of 8.0 ft³ or less are certified by the U.S. Department of Energy (DOE) to be ENERGY STAR-level efficient if they operate at 0.48 kWh/kg energy intensity (i.e., have an Integrated Energy Factor IEF=2.09 L/kWh). Dehumidifiers with a volume over 8.0 ft³ are certified as ENERGY STAR-level efficient if they operate at 0.303 kWh/kg energy intensity (IEF=3.3 L/kWh).

(4) The measured energy demand falls below the latent-heat limit, implying that water is released as clusters or micro-droplets rather than as pure vapor. This mechanism can entrain salt ions and polymer fragments—ranging from nano- to micro-scale—during extraction. Such particles are invisible to routine analytical methods yet still pose potential health risks. Consistent with this picture, the collected water contains 1.5–15.2 ppm of lithium ions, confirming that lithium chloride was carried out of the sorbent together with the harvested water.

We tested the collected water for both presence of salt ions and any polymer residue. During this second round of revisions, we realized that we forgot to include a reference from the main text to **Supplementary Note 8,** which has been added during the first round of revisions. The note is included below. We also added the following text to the discussion section of the revised manuscript.

Scaling up this new extraction technology will necessitate further research into ultrasound-induced degradation of various sorbent materials. The robustness, cyclic stability, and efficacy for long term water harvesting capability of PAM-LiCl HG-A hydrogel composites have been previously demonstrated in numerous works[33–35]. Our initial lab-scale testing confirms that these sorbents maintain structural integrity after multiple piezo actuation cycles, as evidenced by absence of any traces of polymer residue in collected water filtered by a VWR filter paper (see **Supplementary Notes 5,8**). Our observations and spectroscopic analyses (**Supplementary Fig. S26**) also agree with prior independent studies of polymers and hydrogels subjected to piezo actuation, which have demonstrated resilience to vibrational deformations[36,37] and self-healing performance.[38] Similarly, in this work, we did not observe any material degradation or performance loss of either HG-A or HG-M hydrogels during multiple actuation cycles (**Figs. 6a,b** and **Supplementary Figs. S28 and S35**). Degradation resistance of other sorbents will need to be evaluated separately. Some may prove incompatible with this method of extraction, others may need to be re-engineered to improve their mechanical properties so they can withstand vibrational forces over many regeneration cycles.

It should also be noted that a traditional photothermal method of moisture extraction from sorbents also causes their accelerated degradation. For example, solar radiation causes rapid UV-triggered photooxidative degradation of polymers via chain scission and formation of free radicals, [39,40] which for some polymers is further accelerated in the presence of moisture and at higher temperatures.[41–43] Prior studies demonstrated that 368 nm UV irradiation can effectively degrade hydrogels[44]. Likewise, MOFs may also deteriorate under UV and sunshine exposure [45]. Even when the sorbents themselves are not directly exposed to sunlight during the moisture extraction process, long exposure of solar absorbers and constructional elements of the AWH system to sunlight, high temperatures, and moisture accelerate their ageing. Long-term studies of sorbent degradation under various stimuli (sunlight, moisture swings, temperature swings, and ultrasound signals) will need to be done for any sorbent considered for outdoor AWH operation to evaluate their lifetimes under different operational scenarios in real-life applications.

As we mention in the discussion and Supplementary Notes, there are no health recommendations on the Li dose that is safe for human consumption. While some studies suggest the dose should be limited to below 3.1 mg per day[46], other recent publications revel the important role Li plays in preventing Alzheimer's disease and recommend routine usage of Li salts to prevent Li

deficiency[47]. As shown in **Supplementary Fig. S.38,** an average Li content in the water extracted over several cycles was ~6 mg/L, which is within the range of Li content present in bottled water from dozens of countries, previously measured to range from ~0 to 9.9 mg/L [48,49].

It is important to emphasize that the new extraction methodology is equally applicable to Li-free hydrogels (such as e.g. HG-M gels shown in this work) and is expected to be fully compatible with other previously demonstrated sorbents that do not contain salts.

1.8. Supplementary Note 8 – Structural integrity of hydrogel under ultrasonic extraction

To evaluate the structural integrity of the hydrogel and the extracted water quality after desorption, the water extracted from LiCl-PAM hydrogels (HG-A) were filtered using a VWR@ sterile syringe filter, commonly employed for ICP-OES testing. In this experiment, three piezoelectric devices were used to extract water from a ~5.92 g HG-A specimen at a duty cycle of 25-30% over a duration of ~45 min. The setup and test were made and conducted within an enclosed petri dish, respectively. Following desorption, ~0.21 ml of desorbed water was collected from the petri dish lid and subsequently filtered using a VWR filter paper kit to examine for any traces of polymer residue.

The initial dry weight of the filter paper kit was ~2.99 g, which increased to ~3.02 g after the filtration of ~0.21 ml extracted water at 20% relative humidity, resulting in wetting the filter paper. Following drying at room temperature, the weight of the filter paper returned to 2.99 g, with no polymer residue detected. This provides the evidence that hydrogels remained intact following the ultrasonic actuation process, and the extracted water is not contaminated by the polymer.

(5) The long-term stability could be a major challenge in this actuator-hydrogel-based AWH system. Lithium chloride aggressively corrodes most metals, threatening ultrasonic device integrity, so the claimed 25-year service life is almost certainly an overestimate. Equally uncertain is the hydrogel itself: its mechanical strength, degree of polymerization, and resistance to cyclic swelling must be monitored over thousands of operating cycles. The current durability test, only a 25–30 % duty cycle over 45 min, falls far short of demonstrating a 30-day lifespan. These unresolved reliability issues also cast doubt on the projected cost target of \$0.19 L^{-1}

Supplementary Fig. 37a illustrates that – owing to the low cost of hydrogel – its lifespan does not have a noticeable effect on the water costs. Furthermore, **Supplementary Fig. 37b** shows the estimated water costs as a function of the device lifespan in the range from 1 to 45 years. The provided detailed formula and all the variables used in this analysis can be used by the readers to re-evaluate the predicted water cost under different assumptions about the device lifespan and energy costs at a specific location.

We agree with the reviewer in general that long-term stability and performance of any new AWH installation using ultrasound extraction will need to be evaluated separately by performing long-

term testing in the field. The goal of this manuscript is to introduce a new highly-energy efficient method of moisture extraction, which will inspire further studies and device optimization. To not dilute this message, we included a techno-economic analysis into a Supplementary Note only. This analysis was added by the request from several original reviewers and is explicitly referred to as a "Preliminary" to avoid making any strong claims.

As mentioned above, the robustness, cyclic stability, and efficacy for long term water harvesting capability of PAM-LiCl HG-A hydrogel composites have been previously demonstrated in numerous works[33–35]. Similarly, in this work, we did not observe any material degradation or performance loss of either HG-A or HG-M hydrogels during multiple actuation cycles (**Figs. 6a,b** and **Supplementary Figs. S28 and S35**).

The manufacturer-indicated lifespan of piezoelectric actuators used in this study[50] is 45 years. In prior studies, the NASA Jet Propulsion Laboratory conducted life testing on commercial piezoelectric PZT actuators, pre-stressed to 18 MPa, for up to 100 billion cycles over 580 days, revealing no discernible damage or substantial performance decline[51]. Several strategies can be additionally implemented to preserve long lifespans of actuators used in AWH systems. A waterproof silicon-based membrane may replace the metal membrane in the actuator used in this study, maintaining a comparable displacement and velocity profile [52]. Silicon coating over metallic or other corrosion-prone elements can be used to enhance corrosion resistance[53]. Alternatively, corrosion-resistant ultrasonic transducers can be used, e.g., those based on monocrystal fibers [54,55] or on hydrophobic polymers such as polyvinylidene fluoride (PVDF)[56].

Finally, as already mentioned above, the new extraction methodology is equally applicable to Li-free hydrogels (such as e.g. HG-M gels shown in this work) and is expected to be fully compatible with other previously demonstrated sorbents that do not contain salts.

The above paragraphs have been included into the discussion section.

1.6. Supplementary Note 6 – Structural integrity of hydrogel under ultrasonic extraction

To evaluate the structural integrity of the hydrogel and the extracted water quality after desorption, the water extracted from LiCl-PAM hydrogels (HG-A) were filtered using a VWR@ sterile syringe filter, commonly employed for ICP-OES testing. In this experiment, three piezoelectric devices were used to extract water from a ~5.92 g HG-A specimen at a duty cycle of 25-30% over a duration of ~45 min. The setup and test were made and conducted within an enclosed petri dish, respectively. Following desorption, ~0.21 ml of desorbed water was collected from the petri dish lid and subsequently filtered using a VWR filter paper kit to examine for any traces of polymer residue.

The initial dry weight of the filter paper kit was ~2.99 g, which increased to ~3.02 g after the filtration of ~0.21 ml extracted water at 20% relative humidity, resulting in wetting the filter paper. Following drying at room temperature, the weight of the filter paper returned to 2.99 g, with no polymer residue detected. This provides the evidence that hydrogels remained intact

following the ultrasonic actuation process, and the extracted water is not contaminated by the polymer.

(6) Noise pollution represents an additional, often-overlooked challenge, particularly for scaled-up arrays capable of meeting an adult's daily water requirement. A single ultrasonic actuator poses little risk to human health, yet hundreds operating in close proximity can create an ultrasound level that may compromise comfort and well-being; this collective impact must be explicitly evaluated and mitigated.

We illustrated in **Supplementary Figure S24** that there is no ultrasonic noise when AWH sorbents are fully utilized. The acoustic wave is fully absorbed by the hydrogel layer, and its energy is used to extract moisture and heat the sorbent.

References

1. Boriskina, S. V. *et al.* Heat meets light on the nanoscale. *Nanophotonics* **5**, 134–160 (2016).
2. Boriskina, S. V *et al.* Roadmap on optical energy conversion. *Journal of Optics* **18**, 073004 (2016).
3. Wurfel, P. The chemical potential of radiation. *Journal of Physics C: Solid State Physics* **15**, 3967–3985 (1982).
4. Yang, X., Chen, Z., Xiang, C., Shan, H. & Wang, R. Enhanced continuous atmospheric water harvesting with scalable hygroscopic gel driven by natural sunlight and wind. *Nat Commun* **15**, 7678 (2024).
5. Zou, H. *et al.* High-Efficiency Atmospheric Water Harvesting and Irrigation Recycling in Greenhouse Using Hygroscopic Composite Gels. *Adv Funct Mater* **n/a**, 2501163 (2025).
6. Zhao, Y. *et al.* Material-to-system tailored multilayer-cyclic strategy toward practical atmospheric water harvesting. *Proceedings of the National Academy of Sciences* **122**, e2500928122 (2025).
7. Xu, J. *et al.* All-in-one hybrid atmospheric water harvesting for all-day water production by natural sunlight and radiative cooling. *Energy Environ Sci* **17**, 4988–5001 (2024).
8. Badescu, V. Spectrally and angularly selective photothermal and photovoltaic converters under one-sun illumination. *J. Phys. D: Appl. Phys.* **38**, 2166 (2005).
9. McEnaney, K., Kraemer, D. & Chen, G. Direct heat-to-electricity conversion of solar energy. *An. Rev. Heat Transf.* **15**, 179–230 (2012).
10. Bermel, P., Lee, J., Joannopoulos, J. D., Celanovic, I. & Soljacic, M. Selective solar absorbers. *An. Rev. Heat Transf.* (2012).

11. Yeng, Y. X. *et al.* Enabling high-temperature nanophotonics for energy applications. *Proc Natl Acad Sci U S A* **109**, 2280–5 (2012).

12. Boriskina, S. V. *et al.* Roadmap on optical energy conversion. *J. Optics* (2015).

13. McEnaney, K. Modeling of solar thermal selective surfaces and thermoelectric generators. (MIT, 2010).

14. Cooper, T., Zandavi, S. H., Ni, G., Boriskina, S. V. & Chen, G. Contactless steam generation and superheating under one sun illumination. *Nature Communicat.* **9**, 5086 (2018).

15. Ekins-Daukes, N. J., Soeriyadi, A., Zhao, W., Bremner, S. & Pusch, A. Loss analysis for single junction concentrator solar cells. *AIP Conf Proc* **2012**, 40003 (2018).

16. Micha, D. N. & Silvares Junior, R. T. The Influence of Solar Spectrum and Concentration Factor on the Material Choice and the Efficiency of Multijunction Solar Cells. *Sci Rep* **9**, 20055 (2019).

17. Siefer, G. *et al.* Influence of the simulator spectrum on the calibration of multi-junction solar cells under concentration. in *Conference Record of the Twenty-Ninth IEEE Photovoltaic Specialists Conference, 2002.* 836–839 (2002). doi:10.1109/PVSC.2002.1190709.

18. Geisz, J. F. *et al.* 40.8% efficient inverted triple-junction solar cell with two independently metamorphic junctions. *Appl Phys Lett* **93**, 123505 (2008).

19. Fernández, E. F., Siefer, G., Schachtner, M., García Loureiro, A. J. & Pérez-Higueras, P. Temperature coefficients of monolithic III-V triple-junction solar cells under different spectra and irradiance levels. *AIP Conf Proc* **1477**, 189–193 (2012).

20. Xu, J. *et al.* All-in-one hybrid atmospheric water harvesting for all-day water production by natural sunlight and radiative cooling. *Energy Environ Sci* **17**, 4988–5001 (2024).

21. Zou, H. *et al.* High-Efficiency Atmospheric Water Harvesting and Irrigation Recycling in Greenhouse Using Hygroscopic Composite Gels. *Adv Funct Mater* (2025) doi:10.1002/adfm.202501163.

22. Qi, H. *et al.* An Interfacial Solar-Driven Atmospheric Water Generator Based on a Liquid Sorbent with Simultaneous Adsorption–Desorption. *Advanced Materials* **31**, (2019).

23. Wang, J. Y., Liu, J. Y., Wang, R. Z. & Wang, L. W. Experimental investigation on two solar-driven sorption based devices to extract fresh water from atmosphere. *Appl Therm Eng* **127**, 1608–1616 (2017).

24. Fathieh, F. *et al.* Practical water production from desert air. *Sci Adv* **4**, (2018).

25. LaPotin, A. *et al.* Dual-Stage Atmospheric Water Harvesting Device for Scalable Solar-Driven Water Production. *Joule* **5**, 166–182 (2021).

26. Kim, H. *et al.* Adsorption-based atmospheric water harvesting device for arid climates. *Nat Commun* **9**, 1191 (2018).

27. Xu, J. *et al.* Efficient Solar-Driven Water Harvesting from Arid Air with Metal–Organic Frameworks Modified by Hygroscopic Salt. *Angewandte Chemie International Edition* **59**, 5202–5210 (2020).

28. Hanikel, N. *et al.* Rapid Cycling and Exceptional Yield in a Metal-Organic Framework Water Harvester. *ACS Cent Sci* **5**, 1699–1706 (2019).

29. Li, R., Shi, Y., Wu, M., Hong, S. & Wang, P. Improving atmospheric water production yield: Enabling multiple water harvesting cycles with nano sorbent. *Nano Energy* **67**, 104255 (2020).

30. Xu, J. *et al.* Ultrahigh solar-driven atmospheric water production enabled by scalable rapid-cycling water harvester with vertically aligned nanocomposite sorbent. *Energy Environ Sci* **14**, 5979–5994 (2021).

31. Yang, X., Chen, Z., Xiang, C., Shan, H. & Wang, R. Enhanced continuous atmospheric water harvesting with scalable hygroscopic gel driven by natural sunlight and wind. *Nat Commun* **15**, 7678 (2024).

32. Bae, S. & Bae, M. A Study on the Acoustic Analysis of the Dehumidifier in the Home Environment. *Adv Sci Lett* **24**, 708–710 (2018).

33. Lu, H. *et al.* Tailoring the Desorption Behavior of Hygroscopic Gels for Atmospheric Water Harvesting in Arid Climates. *Advanced Materials* **34**, 2205344 (2022).

34. Graeber, G. *et al.* Extreme Water Uptake of Hygroscopic Hydrogels through Maximized Swelling-Induced Salt Loading. *Advanced Materials* **n/a**, 2211783 (2023).

35. Díaz-Marín, C. D. *et al.* Physics-based prediction of moisture-capture properties of hydrogels. *Nat Commun* **15**, 8948 (2024).

36. Venegas-Sanchez, J. A., Tagaya, M. & Kobayashi, T. Effect of ultrasound on the aqueous viscosity of several water-soluble polymers. *Polym J* **45**, 1224–1233 (2013).

37. Shamsipur, M., Taherpour, A. A. & Pashabadi, A. Comprehensive facilitating of water oxidation reaction by ultrasonic attenuation of hydrogen-bonded structure of water. *Ultrason Sonochem* **42**, 381–389 (2018).

38. Zhao, X. *et al.* Active scaffolds for on-demand drug and cell delivery. *Proc Natl Acad Sci U S A* **108**, (2011).

39. Madsen, M. V., Tromholt, T., Norrman, K. & Krebs, F. C. Concentrated light for accelerated photo degradation of polymer materials. *Adv Energy Mater* **3**, (2013).

40. Cai, L., Wang, J., Peng, J., Wu, Z. & Tan, X. Observation of the degradation of three types of plastic pellets exposed to UV irradiation in three different environments. *Science of The Total Environment* **628–629**, 740–747 (2018).

41. Rujnić Havstad, M., Tucman, I., Katančić, Z. & Pilipović, A. Influence of Ageing on Optical, Mechanical, and Thermal Properties of Agricultural Films. *Polymers (Basel)* **15**, (2023).

42. Lundin, T., Cramer, S. M., Falk, R. H. & Felton, C. Accelerated Weathering of Natural Fiber-Filled Polyethylene Composites. *Journal of Materials in Civil Engineering* **16**, (2004).

43. Fernández-González, V., Andrade-Garda, J. M., López-Mahía, P. & Muniategui-Lorenzo, S. Impact of weathering on the chemical identification of microplastics from usual packaging polymers in the marine environment. *Anal Chim Acta* **1142**, 179–188 (2021).

44. Li, R. & Wang, P. Sorbents, processes and applications beyond water production in sorption-based atmospheric water harvesting. *Nature Water* vol. 1 Preprint at https://doi.org/10.1038/s44221-023-00099-0 (2023).

45. Kim, V. *et al.* Copper-Based Two-Dimensional Metal–Organic Frameworks for Fenton-like Photocatalytic Degradation of Methylene Blue under UV and Sunlight Irradiation. *Inorg Chem* **63**, 8832–8845 (2024).

46. Schrauzer, G. N. Lithium: Occurrence, Dietary Intakes, Nutritional Essentiality. *Journal of the American College of Nutrition* **21**, 14–21 (2002).

47. Aron, L. *et al.* Lithium deficiency and the onset of Alzheimer's disease. *Nature* (2025) doi:10.1038/s41586-025-09335-x.

48. KRACHLER, M. & SHOTYK, W. Trace and ultratrace metals in bottled waters: Survey of sources worldwide and comparison with refillable metal bottles. *Science of The Total Environment* **407**, 1089–1096 (2009).

49. Iordache, A. M., Voica, C., Roba, C. & Nechita, C. Lithium Content and Its Nutritional Beneficence, Dietary Intake, and Impact on Human Health in Edibles from the Romanian Market. *Foods* **13**, 592 (2024).

50. PI Ceramic. *Reliability & Lifetime of Multilayer Piezo Actuators*. (2025).

51. Sherrit, S. *et al.* Piezoelectric multilayer actuator life test. *IEEE Trans Ultrason Ferroelectr Freq Control* **58**, 820–828 (2011).

52. Sharma, P. & Jackson, N. Vibration analysis of MEMS vibrating mesh atomizer. *Journal of Micromechanics and Microengineering* **32**, 065007 (2022).

53. Zhao, J., Wang, P., Ma, H., Cheng, X. & Li, X. Essential role of Si in enhancing corrosion resistance of high strength low alloy steels in marine environment. *Journal of Materials Research and Technology* **30**, 3328–3339 (2024).

54. Alves Nogueira, F. E. *et al.* New Piezoelectric Generator (PG) Based on a Lithium Tantalate (LiTaO 3) Monocrystal Fiber. *Cryst Growth Des* **25**, 5330–5337 (2025).

55. Campos, R. V. B. *et al.* High-Performance Piezoelectric Generator Based on a Monocrystalline LiNbO 3 Fiber. *Cryst Growth Des* **25**, 672–679 (2025).

56. Platte, M. PVDF ultrasonic transducers. *Ferroelectrics* **75**, 327–337 (1987).